

Potentialiation of Potassium Currents by Beta-Adrenoceptor Agonists in Human Urinary Bladder Smooth Muscle Cells: A Possible Electrical Mechanism of Relaxation

Jun Takemoto^{a,c} Haruko Masumiya^a Kazuo Nunoki^d Takeya Sato^{a,c}
Haruo Nakagawa^b Yoshihiro Ikeda^b Yoichi Arai^b Teruyuki Yanagisawa^{a,c}

Departments of ^aMolecular Pharmacology and ^bUrology, Graduate School of Medicine, Tohoku University, and ^cTohoku University 21st Century COE Program 'Comprehensive Research and Education Center for Planning of Drug and Clinical Evaluation, CRESCENDO', Sendai, and ^dDepartment of Human Health and Nutrition, Shokei Gakuin University, Natori, Japan

Key Words

Ca²⁺-activated K⁺ (K_{Ca}) channels · Iberiotoxin · Apamin · BRL 37344 · Patch clamp, whole-cell

Abstract

We examined the effects of β -adrenoceptor agonists on the membrane currents of smooth muscle cells from the human urinary bladder using a whole-cell patch clamp to investigate the involvement of Ca²⁺-activated K⁺ (K_{Ca}) channels in relaxation by β -adrenergic agonists. With 0.05 mmol/l EGTA in the patch pipette, depolarizing pulses evoked outward rectifying currents. Isoproterenol (1 μ mol/l) significantly increased the membrane currents by 75% at +80 mV with 0.05 mmol/l EGTA pipette solution. BRL 37344 (1 μ mol/l) significantly increased the membrane currents by 44% at +80 mV. Iberiotoxin (100 nmol/l) significantly decreased the membrane currents by 60% at +80 mV. In the presence of iberiotoxin, the potentiation of the outward currents by isoproterenol was greatly suppressed and, in the presence of iberiotoxin and apamin (1 μ mol/l), the potentiation by isoproterenol was totally abolished. On the other hand, with 5 mmol/l EGTA pipette solution, depolarizing pulses evoked smaller outward currents. Isoproterenol (1 μ mol/l) did not change the membrane currents with 5 mmol/l EGTA pipette

solution. The real-time PCR analysis revealed the expression of β_2 -adrenoceptors in the cells. These results suggest that Ca²⁺-activated and iberiotoxin- and apamin-sensitive currents via both large-conductance and small-conductance K_{Ca} channels could be increased by stimulation of β_2 -adrenoceptors.

Copyright © 2008 S. Karger AG, Basel

Introduction

It has been shown that β -adrenoceptor agonists exert potent relaxant effects on the detrusor muscle of the bladder in various species [1–3] and β -adrenoceptors of the detrusor muscle are a potential therapeutic target for overactive bladder. The effects of β -adrenoceptor agonists on smooth muscle are generally considered to be mediated by intracellular cyclic adenosine monophosphate (cAMP) through stimulation of adenylyl cyclase via stimulatory G protein coupled to the β -adrenoceptors (briefly reviewed by Tanaka et al. [4]) and it has also been suggested that relaxation of the smooth muscles by β -adrenoceptor agonists results from phosphorylation by cAMP-dependent protein kinase (PKA) of the contractile machinery of smooth muscle including myosin light-

KARGER

Fax +41 61 306 12 34
E-Mail karger@karger.ch
www.karger.com

© 2008 S. Karger AG, Basel
0031-7012/08/0813-0251\$24.50/0

Accessible online at:
www.karger.com/pha

Teruyuki Yanagisawa
2-1 Seiryō-machi
Aoba-ku
Sendai, 980-8575 (Japan)
Tel. +81 22 717 8061, Fax +81 22 717 8065, E-Mail yanagiswt@mail.tains.tohoku.ac.jp

chain kinase [5], although some discrepancies exist between the increases in cAMP and the relaxation of canine coronary arterial smooth muscle [6], and between the inhibition of adenylyl cyclase or PKA and that of relaxation of rat urinary bladder [7]. Various recent studies have examined the effects of β -adrenoceptor agonists on the excitability of the membrane and contractility of smooth muscle. It has been shown that the hyperpolarization induced by the opening of various type K^+ channels in smooth muscles results in relaxation, that is 'hyperpolarization-relaxation coupling' [8]. In detrusor smooth muscle cells of guinea pigs, it was suggested that isoproterenol probably hyperpolarized the membrane by stimulating the sodium pump activity and preventing spontaneous action potentials [9]. Kobayashi et al. [10] showed that the relaxation of guinea pig bladder smooth muscle by isoproterenol had a causal relation to the increase in large-conductance Ca^{2+} -activated K^+ (BK_{Ca}) currents subsequent to activation of the cAMP/PKA pathway. It was also shown in guinea pig urinary bladder smooth muscle that BK_{Ca} channels are activated indirectly by β -adrenoceptor agonists through Ca^{2+} influx through voltage-dependent L-type Ca^{2+} channels and Ca^{2+} sparks [11]. However, the effects of β -adrenoceptor stimulation on the membrane currents of smooth muscle cells of human urinary bladder have not been reported.

The β -adrenoceptors of human detrusor muscle were shown not to have functional characteristics typical of β_1 - or β_2 -adrenoceptors [12]. Based on the rank order of the potency of agonists, *in vitro* relaxation studies have demonstrated that the β_3 -adrenoceptor is predominantly involved in the relaxation of human detrusor muscle [13, 14]. With the use of quantitative reverse-transcription polymerase chain reaction (RT-PCR), it has also been demonstrated that human detrusor muscles from normal and obstructed bladders predominantly express β_3 -adrenoceptor messenger RNA (mRNA), although those of β_1 - and β_2 -receptors are expressed at lower levels [15]. Taken together, it seems likely that the subtype of β -adrenoceptors involved in relaxation is predominantly β_3 in human detrusor muscle.

In the present study we examined the effects of isoproterenol and BRL 37344, a β_3 -adrenoceptor agonist with β_2 -adrenoceptor affinity [16, 17], on the membrane currents of smooth muscle cells from human urinary bladder to investigate the possibility that hyperpolarization by an increase in outward Ca^{2+} -activated K^+ (K_{Ca}) current might be involved in the relaxation of the human urinary bladder by β -adrenoceptor stimulation.

Materials and Methods

Cell Culture

Smooth muscle cells of human urinary bladder were obtained from Cambrex Bio Science (Walkersville, Md., USA). The smooth muscle cells were cultured in SmGM-2 medium (Cambrex) containing 5% fetal bovine serum, gentamicin (50 mg/l) and amphotericin B (50 μ g/l) at 37°C under 5% CO_2 . Smooth muscle cells of human urinary bladder between passages 6 and 8 were used for the experiments.

Electrophysiological Recordings

Membrane currents were recorded with a whole-cell voltage clamp method using an amphotericin B perforated patch (90 μ g/ml). Pipettes with a resistance ranging from 5 to 9 M Ω were filled with pipette solution of the following composition (in mmol/l): 110 potassium aspartate, 30 KCl, 10 NaCl, 1 $MgCl_2$, 10 HEPES, and either 0.05 or 5 EGTA (pH 7.30 with KOH). The external solution was of the following composition (in mmol/l): 135 NaCl, 5.4 KCl, 1.8 $CaCl_2$, 1 $MgCl_2$, 5 HEPES, 11.1 glucose (pH 7.35 with NaOH). The liquid junction potential between the pipette and external solution was corrected before the seal formation [18–20]. After the formation of a gigaohm seal, the pipette capacitance was compensated before the membrane currents were recorded. Series resistance was compensated, and currents were filtered at 1 kHz and recorded at a sampling frequency of 5 kHz. Data acquisition and analysis were performed with a patch clamp amplifier (Axopatch 200B, Axon Instruments, Foster City, Calif., USA), a personal computer and pCLAMP software (version 8.0.2, Axon instruments). All experiments were performed at room temperature (23–25°C).

RNA Extraction and Complementary DNA Synthesis and Real Time RT-PCR Analysis

mRNA was purified from the primary cultured human urinary bladder smooth muscle cells using oligo-dT magnetic beads (Miltelny Biotec, Bergisch Gladbach, Germany) according to the manufacturer's protocol. Complementary DNA (cDNA) generated from mRNA used as templates was synthesized by reverse transcription using an oligo-dT primer and Primescript™ reverse transcriptase (Takara Bio, Tokyo, Japan).

Real-time PCR was performed using a 7500 real-time PCR system (Applied Biosystems, Foster City, Calif., USA) with the specific forward and reverse primers and the hybridization probe DNA for each of the human β -adrenoceptor subtypes and human glyceraldehyde-3-phosphate dehydrogenase (GAPDH) mRNAs to determine the copy numbers of the target cDNA in each sample. The reaction conditions used were as follows: 50°C, 2 min, then 94°C, 2 min, and then 45 cycles of 94°C, 30 s, and 60°C, 1 min. Data for the amplification of the target sequence were collected during the 60°C step. The plasmid DNA carrying either the cDNA for each subtype of human β -adrenoceptors [17] or human GAPDH was used as a standard for each assay. Relative quantitation results were measured using the comparative cycle threshold method, whereby the amplification of the gene of interest is normalized to that of the gene encoding GAPDH measured from the same cDNA sample. The sequences of the forward and the reverse primers and the hybridization probes were as follows: 5'-GAC-GACGACGACGACGATGT-3', 5'-CTTGGATTCCGAGGCGA-AGC-TAMRA-3' and 5'-F-FAM-CGGCACGGCTCGTCCAG-

GCTCG-TAMRA-3' for human β_1 -adrenoceptor; 5'-CCTTCT-TGCTGGCACCCAAT-3', 5'-CCAGGACGATGAGAGACATG-AC-3' and 5'-FAM-ATGCCCACCACCCACACCTCGTC-TAM-RA-3' for human β_2 -adrenoceptor; 5'-CGTTACGGCGCAC-TGGTCAC-3', 5'-TGGCTCATGATGGGCGCAAAC-3' and 5'-F-FAM-CGGCACGGCTCGTCCAGGCTCG-TAMRA-3' for hu-man β_3 -adrenoceptor; 5'-CCAAGGTCATCCATGACAACCTT-TG-3', 5'-CGGCCATCACGCCACAG-3' and 5'-FAM-AGTCC-ATGCCATCACTGCCACCCAG-TAMRA-3' for human GAPDH, respectively.

Drugs

Amphotericin B, isoproterenol, iberiotoxin and apamin were purchased from Sigma (St. Louis, Mo., USA). BRL 37344 [(R*,R*)-(\pm)-4-(2-[(2-[3-chlorophenyl]-2-hydroxyethyl)amino]propyl)-phenoxyacetic acid] was purchased from Tocris (Ellisville, Mo., USA). All other chemicals were of the highest grade commercially available. The drugs were added to the bath solution from a stock solution (<1 mmol/l) in distilled water. Amphotericin B was dissolved in 100% dimethyl sulfoxide. The final concentration of dimethyl sulfoxide (0.15%) did not affect the measured electro-physiological parameters.

Statistics

All experimental data are presented as means \pm SEM. The statistical significance of difference between the means was evaluated by 1-way analysis of variance followed by either paired or unpaired t tests; p values less than 0.05 were considered significant.

Results

Effects of Isoproterenol and BRL 37344 on the Membrane Currents of Smooth Muscle Cells from Human Urinary Bladder

The membrane currents of smooth muscle cells from human urinary bladder were elicited by test pulses from a holding potential of -80 mV to voltages between -100 mV and $+80$ mV. Figure 1A shows representative traces of the membrane currents recorded with pipette solution containing 0.05 mmol/l EGTA. Outward membrane currents were activated at -20 mV and were gradually increased with further depolarization until $+80$ mV. The outward currents with prominent fluctuation were maintained during depolarization without distinct inactivation and time-dependent activation.

The effects of isoproterenol on the currents of smooth muscle from human urinary bladder with 0.05 mmol/l EGTA pipette solution were examined. Figure 1A shows the representative traces of membrane currents recorded in the absence and presence of 1 μ mol/l isoproterenol. Isoproterenol increased both inward and outward currents. The current-voltage (I-V) relationships of the membrane currents were obtained by plotting the maximal inward or

outward current density during a test pulse versus the membrane potential. The I-V curves show that isoproterenol increased the maximal membrane current densities at test potentials more positive than -20 mV (fig. 1B). Isoproterenol significantly increased the maximal membrane current densities from 7.18 ± 1.27 to 12.51 ± 2.66 pA/pF at $+80$ mV ($n = 5$, $p = 0.037$). With 0.05 mmol/l EGTA pipette solution, isoproterenol (0.01 – 1 μ mol/l) increased the maximal membrane current densities at $+80$ mV in a concentration-dependent manner (fig. 1C). The increase with 10 μ mol/l isoproterenol tended to be smaller than that with 1 μ mol/l (data not shown).

It has been suggested that the β_3 -adrenoceptor is predominantly involved in the relaxation of human detrusor muscle. We examined whether BRL 37344, a β_2 - and β_3 -adrenoceptor partial agonist, increases the membrane currents of smooth muscle cells of human urinary bladder. With 0.05 mmol/l EGTA pipette solution, 1 μ mol/l BRL 37344 increased both inward and outward currents, especially the membrane current densities at voltages more positive than $+20$ mV (fig. 1D). BRL 37344 (1 or 10 μ mol/l) increased the maximal membrane current densities from 4.06 ± 0.86 to 6.41 ± 1.50 pA/pF ($n = 6$, $p = 0.043$) or from 6.00 ± 2.27 to 8.59 ± 3.02 pA/pF ($n = 5$, $p = 0.060$), respectively at $+60$ mV, and from 7.09 ± 0.83 to 10.51 ± 1.95 pA/pF ($n = 6$, $p = 0.032$) or from 9.28 ± 2.79 to 13.13 ± 3.98 pA/pF ($n = 5$, $p = 0.039$), respectively at $+80$ mV. The percentage increases at $+80$ mV produced by BRL 37344 in 2 concentrations were almost the same, that is $44 \pm 10\%$ ($n = 6$, 1 μ mol/l) and $44 \pm 7\%$ ($n = 5$, 10 μ mol/l), respectively (fig. 1C). The BRL-37344-induced increase in the membrane currents was 59% of that of 1 μ mol/l isoproterenol ($+75 \pm 22\%$, $n = 5$).

These results indicate that both isoproterenol and BRL 37344 increased the membrane currents of the smooth muscle cells, but, the efficacy of BRL 37344 was about one half of that of isoproterenol.

Effects of Iberiotoxin and Apamin on the Membrane Currents

We examined the effects of iberiotoxin, a BK_{Ca} channel blocker, on the membrane currents in the smooth muscle cells and on the potentiation of the outward currents by isoproterenol with 0.05 mmol/l EGTA pipette solution. Figure 2A shows the representative traces of membrane currents in the absence and presence of 100 nmol/l iberiotoxin and with the subsequent addition of 1 μ mol/l isoproterenol. The I-V curves show that iberiotoxin significantly decreased the maximal outward membrane current densities, and subsequent addition of iso-

proterenol significantly increased the attenuated currents at test potentials of +60 mV and +80 mV. The maximal membrane current densities at +80 mV in the absence and the presence of iberiotoxin, and presence of both iberiotoxin and isoproterenol were 10.22 ± 1.85 , 3.86 ± 0.65 , and 5.31 ± 0.77 pA/pF ($n = 6$), respectively. The increase in current was much smaller than the control isoproterenol response. We examined the effects of apamin, a small-conductance Ca^{2+} -activated K^+ (SK_{Ca})

channel blocker, on the membrane currents and on the potentiation of the outward currents by isoproterenol with 0.05 mmol/l EGTA pipette solution. The maximal membrane current densities at +80 mV in the absence and presence of apamin, and the presence of both apamin and isoproterenol were 13.20 ± 2.30 , 10.74 ± 2.01 , and 16.77 ± 3.07 pA/pF, respectively ($n = 5$). Although apamin tended to decrease the outward current, the potentiation by isoproterenol could not be greatly inhibited by

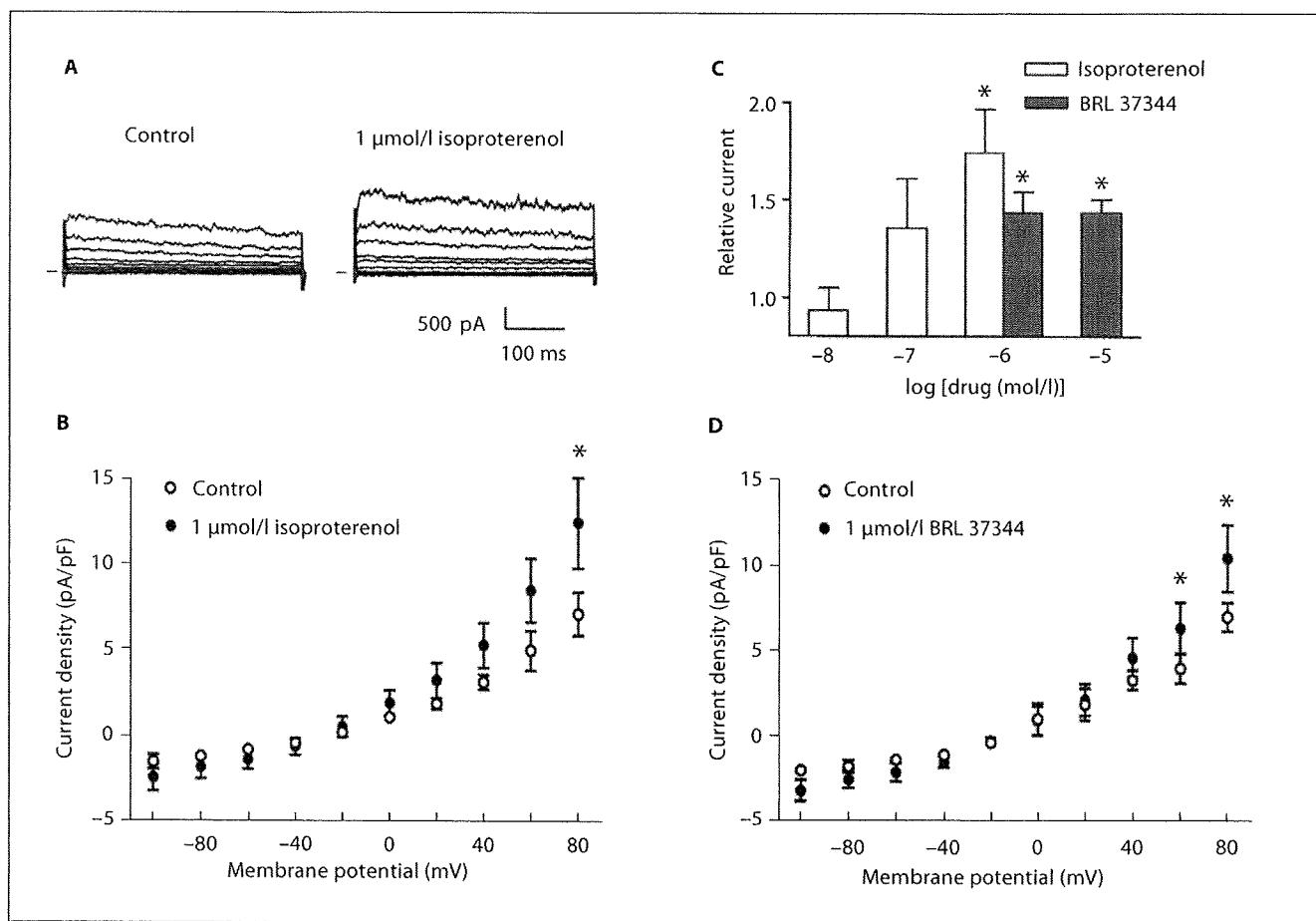


Fig. 1. Isoproterenol and BRL 37344 increased the membrane currents of smooth muscle cells from human urinary bladder. **A** Representative current traces before (left) and during (right) application of 1 μmol/l isoproterenol with low EGTA (0.05 mmol/l) pipette solution. Membrane currents were elicited by 400-ms test pulses from a holding potential of -80 mV to potentials from -100 to +80 in 20-mV steps. Horizontal bars before the current traces indicate zero current level. **B** Current-voltage relationships of membrane currents in the absence (○) and presence (●) of 1 μmol/l isoproterenol. Values indicate means ± SEM of 5 experiments. * $p = 0.037$ versus control. **C** Concentration-response

relationships of isoproterenol and BRL 37344. Membrane currents were elicited by a 400-ms depolarizing test pulse to +80 mV from a holding potential of -80 mV in the absence and presence of each isoproterenol ($n = 5$) and BRL 37344 concentration. Relative currents versus control were calculated. * $p < 0.05$ versus control (1 μmol/l isoproterenol, $n = 5$, $p = 0.037$; 1 μmol/l BRL 37344, $n = 6$, $p = 0.032$; 10 μmol/l BRL 37344, $n = 5$, $p = 0.039$). **D** Current-voltage relationships of membrane currents in the absence (○) and presence (●) of 1 μmol/l BRL 37344 ($n = 6$). * $p < 0.05$ versus control ($p = 0.043$ at +60 mV; $p = 0.032$ at +80 mV).

apamin. Thus, the major part of an increase in the currents by isoproterenol is iberiotoxin sensitive.

We examined the effects of isoproterenol on the currents with patch pipette solution containing 0.05 mmol/l EGTA in the presence of both iberiotoxin and apamin. In the presence of 100 nmol/l iberiotoxin and 1 μ mol/l apamin, the outward current at +80 mV decreased from 13.34 ± 3.70 to 5.66 ± 0.78 pA/pF ($n = 4$), whereas the 1 μ mol/l isoproterenol-induced increase in the current was negated (5.64 ± 1.31 pA/pF, $n = 4$). We also examined the influences of both blockers on the potentiation by isoproterenol. The outward currents at +80 mV in the absence and presence of isoproterenol (1 μ mol/l), and the addition of both iberiotoxin (100 nmol/l) and apamin (1 μ mol/l) on isoproterenol were 7.10 ± 1.79 , 11.15 ± 2.81 , and 4.03 ± 0.29 pA/pF ($n = 4$), respectively.

Therefore, the outward currents potentiated by isoproterenol were iberiotoxin- and apamin-sensitive currents, that is the activation of BK_{Ca} and SK_{Ca} channels via β -adrenoceptors.

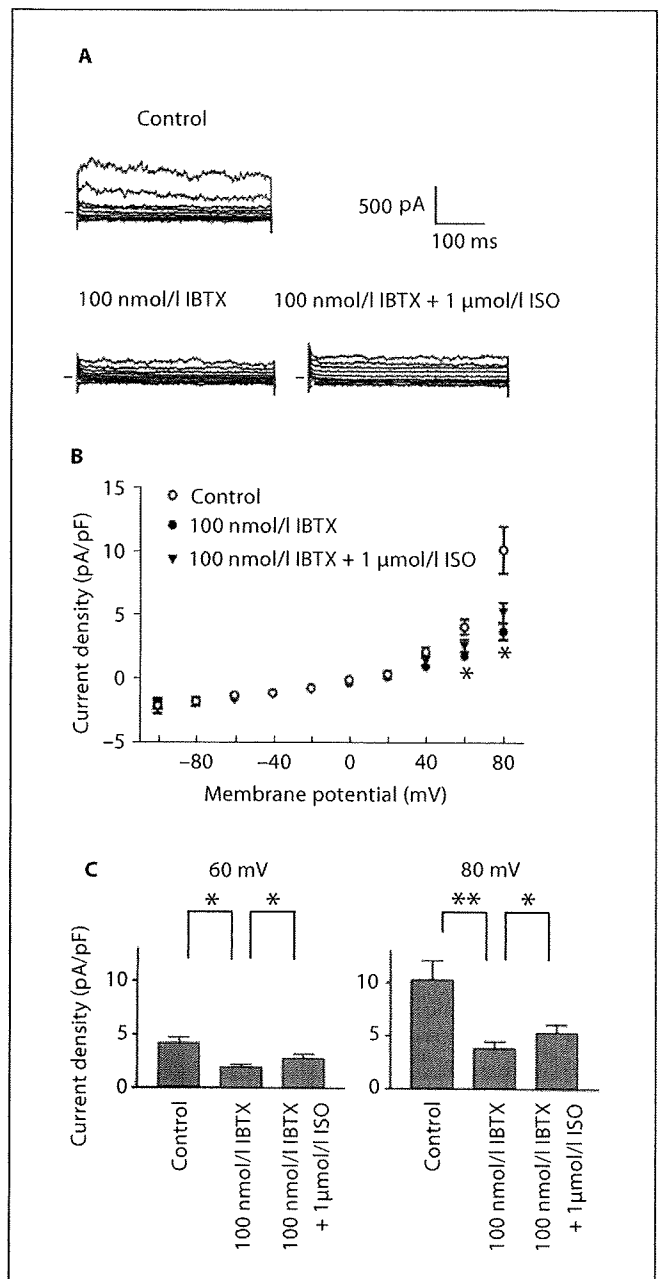
Effects of High Concentration of EGTA on the Membrane Currents

With 5 mmol/l EGTA pipette solution only small outward currents were elicited at +80 mV (fig. 3A). With 0.05 and 5 mmol/l EGTA pipette solutions, the maximal outward membrane current densities at +80 mV were 9.68 ± 1.25 pA/pF ($n = 10$) and 4.70 ± 0.86 pA/pF ($n = 6$, $p = 0.014$), respectively (fig. 3B). With 5 mmol/l EGTA pi-

pette solution, 1 μ mol/l isoproterenol did not affect the membrane currents (fig. 3C). In the absence and presence of 1 nmol/l isoproterenol, the maximal membrane current densities at +80 mV were 4.70 ± 1.05 and 4.80 ± 1.15 pA/pF ($n = 5$), respectively.

These results suggest that the outward currents of smooth muscle cells would be dependent on the increase in the intracellular Ca²⁺ concentration, which would be

Fig. 2. Influences of iberiotoxin (IBTX) on the membrane currents and the potentiation by isoproterenol (ISO). **A** Representative current traces before (upper) and during (lower left) application of 100 nmol/l iberiotoxin and subsequent addition of 1 μ mol/l isoproterenol (lower right) in smooth muscle cells from human urinary bladder. Membrane currents were elicited by 400-ms test pulses from a holding potential of -80 mV to potentials from -100 mV to +80 mV in 20-mV steps. Horizontal bars before the current traces indicate zero current level. **B** Current-voltage relationships of membrane currents in the absence (○) and presence of iberiotoxin (●) and subsequent addition of isoproterenol (▼). Values indicate means \pm SEM of 6 experiments. * $p < 0.05$ between 3 states ($p = 0.010$ at +60 mV; $p = 0.005$ at +80 mV). **C** Current densities in the absence and presence of iberiotoxin and subsequent addition of isoproterenol. Membrane currents were elicited by a 400-ms depolarizing test pulse to +60 mV or +80 mV from a holding potential of -80 mV. * $p < 0.05$ between 2 states and ** $p < 0.01$ between 2 states ($n = 6$; $p = 0.013$ between control and iberiotoxin, $p = 0.033$ between iberiotoxin and subsequent addition of isoproterenol at +60 mV; $p = 0.005$ between control and iberiotoxin, $p = 0.034$ between iberiotoxin and subsequent addition of isoproterenol at +80 mV).



negated by the chelating action of intracellular EGTA at 5 mmol/l. With 5 mmol/l EGTA pipette solution, the membrane currents were not affected by β -adrenoceptor stimulation, so it is suggested that the increase in the outward current by β -adrenoceptor stimulation would be from an increase in K_{Ca} currents. These results indicate that the increase in outward membrane currents by the stimulation of β -adrenoceptors is dependent on the increase in the intracellular Ca^{2+} concentration. Taken together, the major part of the outward membrane currents of smooth muscle cells of human urinary bladder consists of K_{Ca} currents, and the stimulation of β -adrenoceptors increases these currents.

Expression of β -Adrenoceptor mRNA in the Cultured Smooth Muscle Cells from Human Urinary Bladder

To examine the expression of β -adrenoceptors in the cells used in this study, we performed the quantification of the expression levels of each β -adrenoceptor subtype by real-time PCR analysis using a cDNA synthesized from the mRNA used as a template. The quantitative data of expression levels of each β -adrenoceptor subtype, summarized in table 1, revealed that the β_2 -adrenoceptor subtype was predominantly expressed in the smooth muscle cells from human urinary bladder compared to those of both β_1 - and β_3 -adrenoceptor subtypes.

Discussion

In the present study we demonstrated that stimulation of β_2 -adrenoceptors in the smooth muscle cells of human urinary bladder increases the outward current which is

iberiotoxin and apamin sensitive and blocked by intracellular high EGTA. This suggests that K_{Ca} currents are increased by β_2 -adrenoceptor stimulation, resulting in the hyperpolarization and relaxation of the cells.

It has been shown that isoproterenol hyperpolarizes the smooth muscle of the detrusor in guinea pigs via stimulation of β -adrenoceptors [9]. In that study, it was

Fig. 3. Influence of 5 mmol/l EGTA pipette solution on the membrane currents of smooth muscle cells from human urinary bladder. **A** Representative current traces with 0.05 mmol/l (left) or 5 mmol/l (right) EGTA pipette solution. Membrane currents were elicited by 400-ms pulses from a holding potential of -80 mV to test potentials from -100 to $+80$ in 20-mV steps. Horizontal bars before the current traces indicate zero current level. **B** Current-voltage relationships of membrane currents with 0.05 mmol/l (\circ) and 5 mmol/l (\bullet) EGTA pipette solution. Values indicate means \pm SEM of 10 experiments with 0.05 mmol/l and 6 experiments with 5 mmol/l EGTA pipette solution. * $p < 0.05$ versus EGTA 0.05 mmol/l pipette solution ($p = 0.041$ at $+20$ mV; $p = 0.021$ at $+40$ mV; $p = 0.016$ at $+60$ mV; $p = 0.014$ at $+80$ mV). **C** Effects of isoproterenol on the currents recorded with patch pipette solution containing 5 mmol/l EGTA. Current-voltage relationships of membrane currents in the absence (\circ) and presence (\bullet) of $1 \mu\text{mol/l}$ isoproterenol. Values indicate means \pm SEM of 5 experiments.

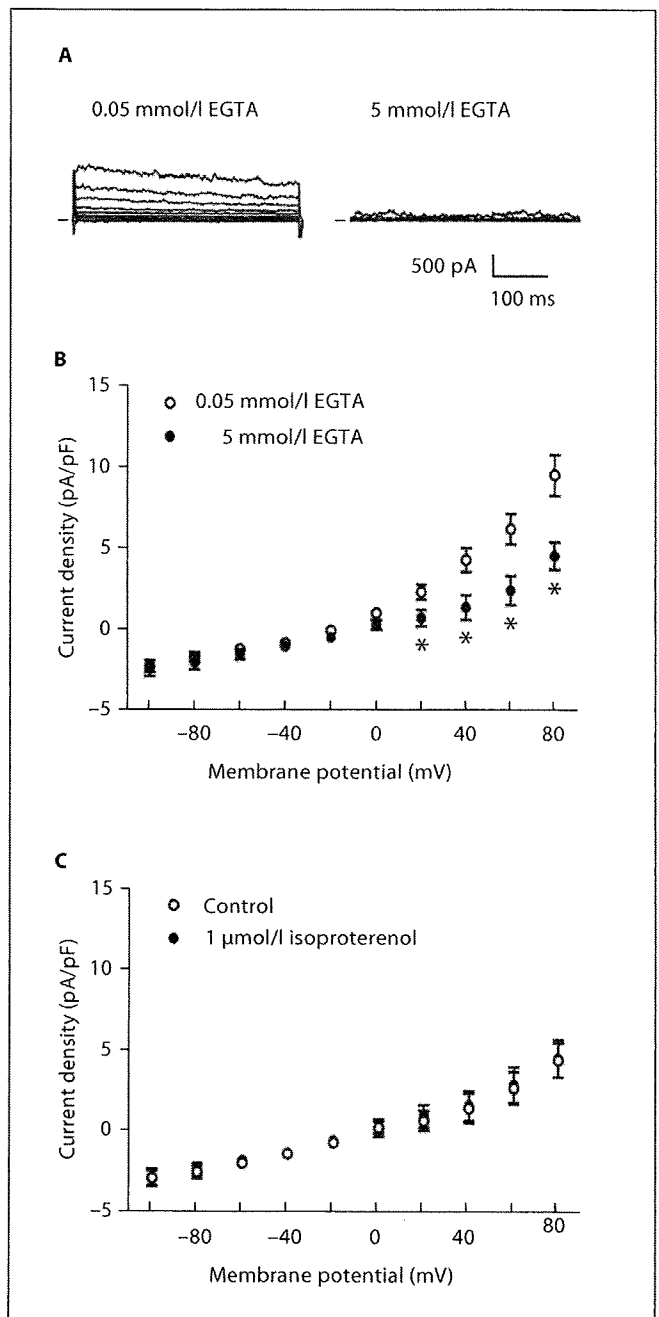


Table 1. Comparison of the expression levels of each β -adrenoceptor subtype in the smooth muscle cells from human urinary bladder by real-time PCR

β -Adrenoceptor subtype	mRNA level normalized by GAPDH mRNA level, $n \times 10^{-6}$
β_1	ND
β_2	2.92 ± 1.10
β_3	ND

Data are expressed as the mean \pm SEM ($n = 5$). ND = Not detected.

suggested that the activity of the sodium pump was facilitated through the cAMP/PKA pathway. It has also been shown by other studies that hyperpolarization of the membrane of the detrusor smooth muscle could be induced through activation of various K^+ channels. Voltage-dependent K^+ channels [21], ATP-sensitive K^+ channels [22], K_{Ca} channels [23] and TREK-1 ($K_{2p2.1}$) channels [24] have been identified in the human detrusor muscle. Using knockout mice, it was shown that the BK_{Ca} channel plays an important role in slowing the excitability and contractility of the detrusor smooth muscle [25]. It was also shown that NS-1619, a BK_{Ca} channel opener, has a relaxant effect on guinea pig bladder smooth muscle [26]. Among the K^+ channels identified in the smooth muscle, the ATP-sensitive K^+ channel is known to be modulated by stimulation of β -adrenoceptors [27]. Kobayashi et al. [10] also showed that isoproterenol and forskolin facilitated iberiotoxin-sensitive BK_{Ca} channels in the smooth muscle cells from the urinary bladder of guinea pigs. The membrane currents potentiated by β -adrenoceptor agonists observed in the present study were voltage- and intracellular Ca^{2+} -dependent outward currents and also iberiotoxin and apamin sensitive. Therefore, it is likely that K_{Ca} currents are potentiated by β -adrenoceptor stimulation in the smooth muscle cells of human urinary bladder. In guinea-pigs' urinary bladder muscles, it was shown that stimulation of β -adrenoceptors activates BK_{Ca} channels by elevating Ca^{2+} influx through voltage-dependent Ca^{2+} channels and by increasing Ca^{2+} sparks [11]. In rat urinary bladder smooth muscle, β_2 -adrenoceptors can simultaneously interact with both BK_{Ca} and L-type Ca^{2+} channels in vivo, which enables the assembly of a unique, highly localized signal transduction complex that mediates the Ca^{2+} - and phosphorylation-dependent modulation of the BK_{Ca} current [28]. In human urinary bladder smooth muscle, the β_2 -adrenoceptor in the sig-

naling complex seems to work like it does in rats. The BK_{Ca} channel interactions with its surrounding signaling partners and its targeting to cell-specific microdomains have been briefly reviewed [29]. To our knowledge, we have shown for the first time that β -adrenoceptor stimulation increases the BK_{Ca} and SK_{Ca} currents of the smooth muscle cells of human urinary bladder. An increase in the BK_{Ca} and SK_{Ca} currents of the human bladder smooth muscle cells by β -adrenoceptor agonists could hyperpolarize the muscle cells, leading to the inhibition of excitation, and the relaxation of the urinary detrusor muscle.

It is well known that isoproterenol relaxes human detrusor muscle [2]. There have been many functional studies on the β -adrenoceptor subtypes mediating relaxation of the urinary bladder. In rabbit bladder it was demonstrated that relaxation of the detrusor muscle is predominantly mediated by β_2 -adrenoceptors. It was also proposed that β_2 - and β_3 -adrenoceptors are involved in the relaxation of rat urinary bladder [30]. A limited number of studies have also suggested the predominant involvement of β_3 -adrenoceptors in the relaxation of the urinary bladder in dogs [30, 31] and monkeys [32]. The functional studies have demonstrated that the β_3 -adrenoceptor is an important subtype for relaxation in the human bladder [13–15, 33–36] followed by the β_2 -adrenoceptor [37]. Studies using PCR, Northern blots and in situ hybridization have detected mRNAs for the β_1 -, β_2 - and β_3 -adrenoceptor subtypes in the human bladder [13, 14, 38]. Although it appears that more than 95% of all β -adrenoceptor mRNAs are the β_3 -subtype in the human bladder, based upon quantitative PCR experiments [15], in the cultured smooth muscle cells of human urinary bladder, β_2 -adrenoceptor mRNAs were detected as a predominant subtype in this study. Therefore, it is probable that isoproterenol and BRL 37344 increase the outward current via stimulation of β_2 -adrenoceptors in the cultured smooth muscle cells.

Using cultured cells of human detrusor muscle with patch clamp methods, we have shown that stimulation of β_2 -adrenoceptors increases the outward currents involved in BK_{Ca} and SK_{Ca} channels, which are important for the stabilization and relaxation of the muscle.

Acknowledgment

This study was supported by the Grants-in-Aid for Scientific Research from the Uehara Memorial Foundation and the Ministry of Education, Science, Sport and Culture, Japan (18613001).

References

- ▶1 Edvardsen P, Setekleiv J: Distribution of adrenergic receptors in the urinary bladder of cats, rabbits and guinea pigs. *Acta Pharmacol Toxicol* 1968;26:437-445.
- ▶2 Nergardh A, Boreus LO: Autonomic receptor function in the lower urinary tract of man and cat. *Scand J Urol Nephrol* 1972;6:32-36.
- ▶3 Elmer M: Inhibitory β -adrenoceptors in the urinary bladder of rat. *Life Sci* 1974;15:273-280.
- ▶4 Tanaka Y, Horinouchi T, Koike K: New insight into β -adrenoceptors in smooth muscle: distribution of receptor subtypes and molecular mechanisms triggering muscle relaxation. *Clin Exp Pharmacol Physiol* 2005;32:503-514.
- ▶5 Andersson KE, Arner A: Urinary bladder contraction and relaxation: physiology and pathophysiology. *Physiol Rev* 2004;84:935-986.
- ▶6 Yamagishi T, Yanagisawa T, Satoh K, Taira N: Relaxant mechanisms of cyclic AMP-increasing agents in porcine coronary artery. *Eur J Pharmacol* 1994;251:253-262.
- ▶7 Frazier EP, Mathy MJ, Peters SLM, Michel MC: Does cyclic AMP mediate rat bladder relaxation by isoproterenol? *J Pharmacol Exp Ther* 2005;313:260-267.
- ▶8 Yanagisawa T, Yamagishi T, Okada Y: Hyperpolarization induced by the K^+ channel openers inhibits Ca^{2+} influx and Ca^{2+} release in coronary artery. *Cardiovasc Drugs Ther* 1993;7:565-574.
- ▶9 Nakahira Y, Hashitani H, Fukuta H, Sasaki S, Kohri K, Suzuki H: Effects of isoproterenol on spontaneous excitation in detrusor smooth muscle cells of the guinea pig. *J Urol* 2001;166:335-340.
- ▶10 Kobayashi H, Adachi-Akahane S, Nagao T: Involvement of BK_{Ca} channels in the relaxation of detrusor muscle via β -adrenoceptors. *Eur J Pharmacol* 2000;404:231-238.
- ▶11 Petkov GV, Nelson MT: Differential regulation of Ca^{2+} -activated K^+ channels by β -adrenoceptors in guinea pig urinary bladder smooth muscle. *Am J Physiol Cell Physiol* 2005;288:C1255-C1263.
- ▶12 Nergardh A, Boreus LO, Naglo A-S: Characterization of the adrenergic β -receptor in the urinary bladder of man and cat. *Acta Pharmacol Toxicol* 1977;40:14-21.
- ▶13 Igawa Y, Yamazaki Y, Takeda H, Hayakawa K, Akahane M, Ajisawa Y, Yoneyama T, Nishizawa O, Andersson KE: Functional and molecular biological evidence for a possible β_3 -adrenoceptor in the human detrusor muscle. *Br J Pharmacol* 1999;126:819-825.
- ▶14 Takeda M, Obara K, Mizusawa T, Tomita Y, Arai K, Tsutsui T, Hatano A, Takahashi K, Nomura S: Evidence for β_3 -adrenoceptor subtypes in relaxation of the human urinary bladder detrusor: analysis by molecular biological and pharmacological methods. *J Pharmacol Exp Ther* 1999;288:1367-1373.
- ▶15 Nomiya M, Yamaguchi O: A quantitative analysis of mRNA expression of α_1 and β -adrenoceptor subtypes and their functional roles in human normal and obstructed bladders. *J Urol* 2003;170:649-653.
- ▶16 Arch JSK, Kaumann AJ: β_3 and atypical β -adrenoceptors. *Med Res Rev* 1993;13:663-729.
- ▶17 Yanagisawa T, Sato T, Yamada H, Sukegawa J, Nunoki K: Selectivity and potency of agonists for the three subtypes of cloned human β -adrenoceptors expressed in Chinese hamster ovary cells. *Tohoku J Exp Med* 2000;192:181-193.
- ▶18 Masumiya H, Tsujikawa H, Hino N, Ochi R: Modulation of manganese currents by 1,4-dihydropyridines, isoproterenol and forskolin in rabbit ventricular cells. *Pflugers Arch* 2003;446:695-701.
- ▶19 MacDonnell KL, Severson DL, Giles WR: Depression of excitability by sphingosine 1-phosphate in rat ventricular myocytes. *Am J Physiol Heart Circ Physiol* 1998;275:H2291-H2299.
- ▶20 Neher E: Correctin for liquid junction potentials in patch clamp experiments. *Methods Enzymol* 1992;297:123-131.
- ▶21 Davies AM, Batchelor TJP, Eardley I, Beech DJ: Potassium channel $K_{v}\alpha 1$ subunit expression and function in human detrusor muscle. *J Urol* 2002;167:1881-1886.
- ▶22 Buckner SA, Milicic I, Daza A, Davies-Taber R, Scott VES, Sullivan JP, Brioni JD: Pharmacological and molecular analysis of ATP-sensitive K^+ channels in the pig and human detrusor. *Eur J Pharmacol* 2000;400:287-295.
- ▶23 Montgomery BSI, Fry CH: The action potential and membrane currents in isolated human detrusor smooth muscle cells. *J Urol* 1992;147:176-184.
- ▶24 Tertysnikova S, Knox RJ, Plym MJ, Thalody G, Griffin C, Neelands T, Harden DG, Singor L, Weaver D, Myers RA, Lodge NJ: BL-1249 [(5,6,7,8-tetrahydro-naphthalen-1-yl)-(2-[1H-tetrazol-5-yl]-phenyl)amine]: a putative potassium channel opener with bladder-relaxant properties. *J Pharmacol Exp Ther* 2005;313:250-259.
- ▶25 Meredith AL, Thorneloe KS, Werner ME, Nelson MT, Aldrich RW: Overactive bladder and incontinence in the absence of the BK large conductance Ca^{2+} -activated K^+ channel. *J Biol Chem* 2004;279:36746-36752.
- ▶26 Malysz J, Buckner SA, Daza AV, Milicic I, Perez-Medrano A, Gopalakrishnan M: Functional characterization of large conductance calcium-activated K^+ channel openers in bladder and vascular smooth muscle. *Naunyn Schmiedeberg Arch Pharmacol* 2004;369:481-489.
- ▶27 Hudman D, Elliott RA, Norman RI: K_{ATP} channels mediate the β_2 -adrenoceptor agonist-induced relaxation of rat detrusor muscle. *Eur J Pharmacol* 2000;397:169-176.
- ▶28 Liu G, Shi J, Yang L, Cao L, Park SM, Cui J, Marx SO: Assembly of a Ca^{2+} -dependent BK channel signaling complex by binding to β_2 adrenergic receptor. *EMBO J* 2004;23:2196-2205.
- ▶29 Lu R, Alioua A, Kumar Y, Eghbali M, Stefani E, Toro L: MaxiK channel partners: physiological impact. *J Physiol* 2006;570:65-72.
- ▶30 Yamazaki Y, Takeda H, Akahane M, Igawa Y, Nishizawa O, Ajisawa Y: Species differences in the distribution of β -adrenoceptor subtypes in bladder smooth muscle. *Br J Pharmacol* 1998;124:593-599.
- ▶31 Takeda H, Matsuzawa A, Igawa Y, Yamazaki Y, Kaidoh K, Akahane S, Kojima M, Miyata H, Akahane M, Nishizawa O: Functional characterization of β -adrenoceptor subtypes in the canine and rat lower urinary tract. *J Urol* 2003;170:654-658.
- ▶32 Takeda H, Yamazaki Y, Akahane M, Akahane S, Miyata H, Igawa Y, Nishizawa O: Characterization of β -adrenoceptor subtype in bladder smooth muscle of cynomolgus monkey. *Jpn J Pharmacol* 2002;88:108-113.
- ▶33 Igawa Y, Yamazaki Y, Takeda H, Akahane M, Ajisawa Y, Yoneyama T, Nishizawa O: Possible β_3 -adrenoceptor-mediated relaxation of the human detrusor. *Acta Physiol Scand* 1998;164:117-118.
- ▶34 Igawa Y, Yamazaki Y, Takeda H, Kaidoh K, Akahane M, Ajisawa Y, Yoneyama T, Nishizawa O, Andersson KE: Relaxant effects of isoproterenol and selective β_3 -adrenoceptor agonists on normal, low compliant and hyperreflexic human bladders. *J Urol* 2001;165:240-244.
- ▶35 Morita T, Iizuka H, Iwata T, Kondo S: Function and distribution of β_3 -adrenoceptors in rat, rabbit and human urinary bladder and external urethral sphincter. *J Smooth Muscle Res* 2000;36:21-32.
- ▶36 Badawi JK, Uecelehan H, Hatzinger M, Michel MS, Haferkamp A, Bross S: Relaxant effects of β -adrenergic agonists on porcine and human detrusor muscle. *Acta Physiol Scand* 2005;185:151-159.
- ▶37 Badawi JK, Seja T, Uecelehan H, Honeck P, Kwon S-T, Bross S, Langbein S: Relaxation of human detrusor muscle by selective β_2 and β_3 agonists and endogenous catecholamines. *Urology* 2007;69:785-790.
- ▶38 Fujimura T, Tamura K, Tsutsumi T, Yamamoto T, Nakamura K, Koibuchi Y, Kobayashi M, Yamaguchi O: Expression and possible functional role of the β_3 -adrenoceptor in human and rat detrusor muscle. *J Urol* 1999;161:680-685.



CLIC4 interacts with histamine H3 receptor and enhances the receptor cell surface expression

Kay Maeda^{a,b,1}, Mitsuya Haraguchi^{a,c,1}, Atsuo Kuramasu^d, Takeya Sato^{a,b},
Kyohei Ariake^e, Hiroyuki Sakagami^f, Hisatake Kondo^g, Kazuhiko Yanai^d,
Kohji Fukunaga^{b,c}, Teruyuki Yanagisawa^{a,b}, Jun Sukegawa^{a,b,*}

^a Department of Molecular Pharmacology, Tohoku University Graduate School of Medicine, Sendai 980-8575, Japan

^b Tohoku University 21st Century COE Program "CRESCENDO", Sendai 980-8575, Japan

^c Department of Pharmacology, Graduate School of Pharmaceutical Sciences, Tohoku University, Sendai 980-8578, Japan

^d Department of Pharmacology, Tohoku University Graduate School of Medicine, Sendai 980-8575, Japan

^e Department of Gastroenterological Surgery, Tohoku University Graduate School of Medicine, Sendai 980-8575, Japan

^f Department of Anatomy, Kitasato University School of Medicine, Sagami-hara 228-8555, Japan

^g Department of Cell Biology, Tohoku University Graduate School of Medicine, Sendai 980-8575, Japan

Received 12 February 2008

Available online 25 February 2008

Abstract

Histamine H3 receptor (H3R), one of G protein-coupled receptors (GPCRs), has been known to regulate neurotransmitter release negatively in central and peripheral nervous systems. Recently, a variety of intracellular proteins have been identified to interact with carboxy (C)-termini of GPCRs, and control their intracellular trafficking and signal transduction efficiencies. Screening for such proteins that interact with the C-terminus of H3R resulted in identification of one of the chloride intracellular channel (CLIC) proteins, CLIC4. The association of CLIC4 with H3R was confirmed in *in vitro* pull-down assays, coimmunoprecipitation from rat brain lysate, and immunofluorescence microscopy of rat cerebellar neurons. The data from flowcytometric analysis, radioligand receptor binding assay, and cell-based ELISA indicated that CLIC4 enhanced cell surface expression of wild-type H3R, but not a mutant form of the receptor that failed to interact with CLIC4. These results indicate that, by binding to the C-terminus of H3R, CLIC4 plays a critical role in regulation of the receptor cell surface expression.

© 2008 Elsevier Inc. All rights reserved.

Keywords: G protein-coupled receptor; Histamine H3 receptor; CLIC4; Trafficking

Histamine regulates numerous functions of central and peripheral nervous systems, including sleep-wake cycle, arousal, cognition, memory, and pain processing, through four receptor subtypes: H1, H2, H3 and H4 [1]. H3R has

been known to inhibit synaptic release of a variety of neurotransmitters including histamine, acetylcholine, dopamine, noradrenaline, glutamate, γ -aminobutyric acid (GABA) [2]. Accordingly, H3R has attracted considerable interest from many pharmaceutical companies as a potential drug target for treatment of various pathological states including neuropathic pain and Alzheimer's disease [1].

In recent years, a growing number of cellular molecules have been identified to interact with C-terminal cytoplasmic domain of GPCR, and in most cases these interactions have been implicated in targeting, intracellular trafficking and subsequent signaling of GPCR [3]. Our previous work also showed that cell surface expression of PTH/PTH-

Abbreviations: CLIC4, chloride intracellular channel 4; ELISA, enzyme-linked immunosorbent assay; GPCR, G protein-coupled receptor; GST, glutathione-S-transferase; H3R, histamine H3 receptor; MBP, maltose binding protein.

* Corresponding author. Address: Department of Molecular Pharmacology, Tohoku University Graduate School of Medicine, Sendai 980-8575, Japan. Fax: +81 22 717 8065.

E-mail address: jsukegaw@mail.tains.tohoku.ac.jp (J. Sukegawa).

¹ These authors contributed equally to this work.

related protein receptor is regulated by interaction of its C-terminal domain with some cellular molecule [4]. With the advancement of the research, it is now becoming increasingly clear that intracellular trafficking and subcellular localization of GPCRs are regulated in elaborate detail through these interactions [5].

CLIC4 belongs to CLIC protein family that consists of seven highly homologous proteins: CLIC1-4, 5A, 5B (p64), and 6 (parchorin). These proteins are widely expressed in multicellular organisms and implicated in anion transport within various subcellular compartments. Among them, however, only CLIC1, CLIC4, and CLIC5 have been shown directly to display anion channel activities in reconstituted planar lipid bilayer systems, albeit with poor selectivity [6]. CLIC proteins share a core structural domain of approximate 240 amino acid residues with a single trans-membrane domain. A crystal structure study on CLIC4 revealed that the core domain of this protein family has a feature as the omega class glutathione-S-transferase proteins, and pointed to the structural foundation of the ability of this domain to conformationally transform itself from a soluble globular protein to an integral membrane protein [7]: an unusual feature shared among CLIC family proteins to “autoinsert” themselves into membranes [8]. CLIC4 has been reported to locate in membrane systems including endoplasmic reticulum (ER), caveola and *trans*-Golgi network, mitochondrial inner membrane, dense core secretory vesicles, and plasma membrane [8]. A study on the CLIC-related protein EXC-4 in *Caenorhabditis elegans* indicated that the protein is indispensable for lumen formation of excretory tube of the nematode [9]. It is also reported that CLIC4 is essential for tubular morphogenesis of cultured human endothelial cells [10]. While other reports suggest that CLIC4 associates with a variety of cellular proteins including dynamin I, 14-3-3 proteins, and rhodopsin [11,12], biological roles of these interactions are largely unknown.

Adding to the reported functional diversity, we present here a new observation that CLIC4 exerts a critical influence on H3R cell surface expression through binding to the C-terminal cytoplasmic domain of the receptor.

Materials and methods

Cell culture. CHO and PC12 cells were grown in DMEM supplemented with 10% FCS, and with 10% horse serum and 5% FCS, respectively. These cells were obtained from Cell Resource Center for Biomedical Research, Tohoku University (Sendai, Japan).

Yeast two-hybrid screening. The screening was carried out using the ProQuest Two-Hybrid System (Invitrogen, CA, USA) according to the manufacturer's recommendation.

In vitro pull-down experiment. The plasmid encoding GST-fused H3R (amino acids 414–445) was constructed from pGEX-5X-2 plasmid (GE Healthcare, UK). The coding sequence for CLIC4 (amino acids 56–253) obtained in the screening was inserted into pMAL-c2 vector (New England BioLabs, MA, USA) to generate MBP-CLIC4 fusion protein. The point mutations of H3R were generated with the aid of QuickChange site-directed mutagenesis kit (Stratagene, CA, USA). Cleared lysates of *Escherichia coli* containing GST-H3R or MBP-CLIC4 fusion protein were

mixed and incubated for 1 h. After further incubated with glutathione-Sepharose 4B (GE Healthcare) for 1 h, proteins associated with the beads were separated on SDS-PAGE and probed with anti-MBP antibody (Cell Signaling Technology, MA, USA). Signals were visualized by HRP-conjugated secondary antibody and ImmunStar HRP substrate (Bio-Rad Laboratories, CA, USA).

Antibody production and immunoprecipitation. A recombinant CLIC4 protein (amino acids 56–253) was used to raise mouse anti-CLIC4 antibody. The antibody was affinity purified by using MicroLink protein coupling gel (Pierce, IL, USA). For production of H3R specific antibody, rabbits were immunized with GST-fused N-terminal domain of H3R (amino acids 1–30), and affinity purified by using MBP-H3R(1–30). Immunoprecipitation was performed as described [13].

Generation of recombinant adenoviruses. The recombinant adenoviruses (rAd-CLIC4, rAd-H3R, rAd-H3RF419A, and rAd- β gal) were generated from pAxCawtit cosmid vector (Nippon Gene, Japan) according to manufacturer's recommendation. In all experiments, total number of viruses was adjusted by adding rAd- β gal expressing β -galactosidase.

Primary culture. Cerebella of E17 Wistar rat embryos were dissected according to protocols provided by Sumitomo Bakelite Co., Ltd. (Tokyo, Japan). Cerebellar cells cultured on poly-D-lysine/laminin-coated coverslips were subjected to immunofluorescence analysis on 22 days *in vitro*. All experimental procedures were complied with the Animals (Scientific Procedures) Act 1986 and the guidelines of the Ministry of Health, Labour and Welfare of Japan, and approved by Institute for Animal Experimentation Tohoku University Graduate School of Medicine.

Immunofluorescence microscopy. PC12 cells plated on coverslips pre-coated with collagen type IV were coinfecting with rAd-H3R (MOI = 2) and rAd-CLIC4 (MOI = 100). Forty-eight hours after infection, cells were fixed in phosphate buffered saline (PBS) containing 4% paraformaldehyde (PFA). After blocking in PBS containing 20% normal goat serum, the cells were incubated with anti-H3R antibody. To locate intracellular CLIC4, cells were permeabilized with 0.1% Triton X-100 in PBS, and incubated with anti-CLIC4 antibody. Cells were then incubated with Alexa Fluor 546-conjugated anti-rabbit and Alexa Fluor 488-conjugated anti-mouse antibodies (Invitrogen), and inspected by Digital Eclipse C1 confocal microscope (Nikon, Japan). Cerebellar cells were fixed in 4% PFA in PBS, and then in cold methanol. Cells were permeabilized with 0.2% Triton X-100 in PBS, and blocked in 1% blocking reagent (TSA kit, Invitrogen). Blocked cells were incubated with anti-H3R and anti-CLIC4 antibodies, and then with Alexa Fluor 546-conjugated anti-rabbit antibody, HRP-conjugated anti-mouse antibody (Cell Signaling Technology), Alexa Fluor 488 tyramide (TSA kit), and Alexa Fluor 647-conjugated anti-calbindin D-28K antibody.

Flow cytometry. Cell surface H3R of PC12 cells coinfecting with rAd-H3R (MOI = 2) and rAd-CLIC4 was labeled with anti-H3R antibody, followed by Alexa Fluor 488-conjugated anti-rabbit antibody. Cell-associated fluorescence was detected by a BD FACSCalibur flow cytometer (BD Biosciences, CA, USA). To measure whole cell H3R expression, the cells were permeabilized with 0.1% Triton X-100 in PBS. All data were analyzed with CellQuest software (BD Biosciences).

Radioligand receptor binding assay. PC12 cells infected with rAd-H3R (MOI = 2) and rAd-CLIC4 were incubated for 1 h in binding buffer (50 mM Tris-HCl, pH 7.4, and 5 mM EDTA) with 2 nM [3 H]-(R)-(-)- α -methylhistamine ([3 H]-RaMH), a selective H3R agonist. After the cells were separated and washed on glass fiber filters, the cell-associated radioactivity was measured. Nonspecific binding was defined as ligand binding in the presence of 10 μ M unlabeled RaMH. Saturation experiments were conducted at five concentrations of [3 H]-RaMH from 5 to 500 nM by using PC12 cells infected with rAd-H3R (MOI = 2) and rAd-CLIC4 (MOI = 0 or 30). Curve fitting was made with GraphPad Prism version 4.00 (GraphPad Software Inc., USA).

Cell-based ELISA. CHO cells infected with rAd-H3R (MOI = 2) or rAd-H3RF419A (MOI = 2) and rAd-CLIC4 were seeded on collagen I-coated 24-well plates. Forty-eight hours after infection, cells were fixed in 4% PFA in PBS and blocked in PBS containing 5% fat-free milk. Cell surface H3R was detected with anti-H3R antibody, and HRP-conjugated anti-rabbit secondary antibody, followed by OPD colorimetric assay.

Wild-type CHO cells with no viral infection were used as negative control. To determine the total amount of H3R in cells, cells were permeabilized with 0.05% Tween 20 in PBS preceding the assay.

Results

Identification of CLIC4 as an H3R interacting protein

Screening of a human brain cDNA library with the C-terminus of H3R (amino acids 414–445) resulted in identification of a clone that harbored the coding sequence for amino acids 56–253 of CLIC4. To confirm the physical interaction of H3R with CLIC4, *in vitro* pull-down assays were performed with GST-H3R and MBP-CLIC4 fusion proteins. As shown in Fig. 1A, MBP-CLIC4 was coprecipitated strongly with GST-H3R C-terminus (414–445). While GST-H3R(414–436) also demonstrated strong interaction with MBP-CLIC4, other fusion proteins, GST-H3R(424–436), (414–423), and (421–427) showed no interaction. These results indicate that the 23 amino acid stretch from 414 to 436 of H3R is responsible for binding to CLIC4. As Chuang et al. showed that CLIC4 interacted also with the C-terminus of rhodopsin [12], we aligned the amino acid sequence 414–436 of H3R with that of the C-terminus of rhodopsin. The comparison showed that F419, R420 and K431 of H3R are shared with rhodopsin in comparable positions (Fig. 1B, upper panel). In order to see if these residues of H3R are involved in binding to CLIC4, we replaced each one or combinations of these residues with alanines. *In vitro* pull-down assays revealed that H3R F419A, FR/AA, and FRK/AAA completely lost the binding activities, indicating that F419 is critically important for H3R to interact with CLIC4 (Fig. 1B, lower panel). As for CLIC4, MBP-CLIC4 C-terminus (56–253) and MBP-CLIC4(121–253) interacted strongly with GST-H3R, but other subsegments of CLIC4 showed only minimum interactions with GST-H3R (Fig. 1C). These results indicate that the H3R binding domain of CLIC4 extends widely from amino acids 121 to 253.

In vivo association of CLIC4 with H3R

The association of CLIC4 with H3R was studied in PC12 cells transiently expressing both H3R and CLIC4. Immunofluorescence microscopy showed overlapping localizations of the two proteins at the plasma membrane (Fig. 2A). Then, immunoprecipitation experiments using P2 fraction of rat brain homogenates revealed that endogenous CLIC4 was coimmunoprecipitated with H3R

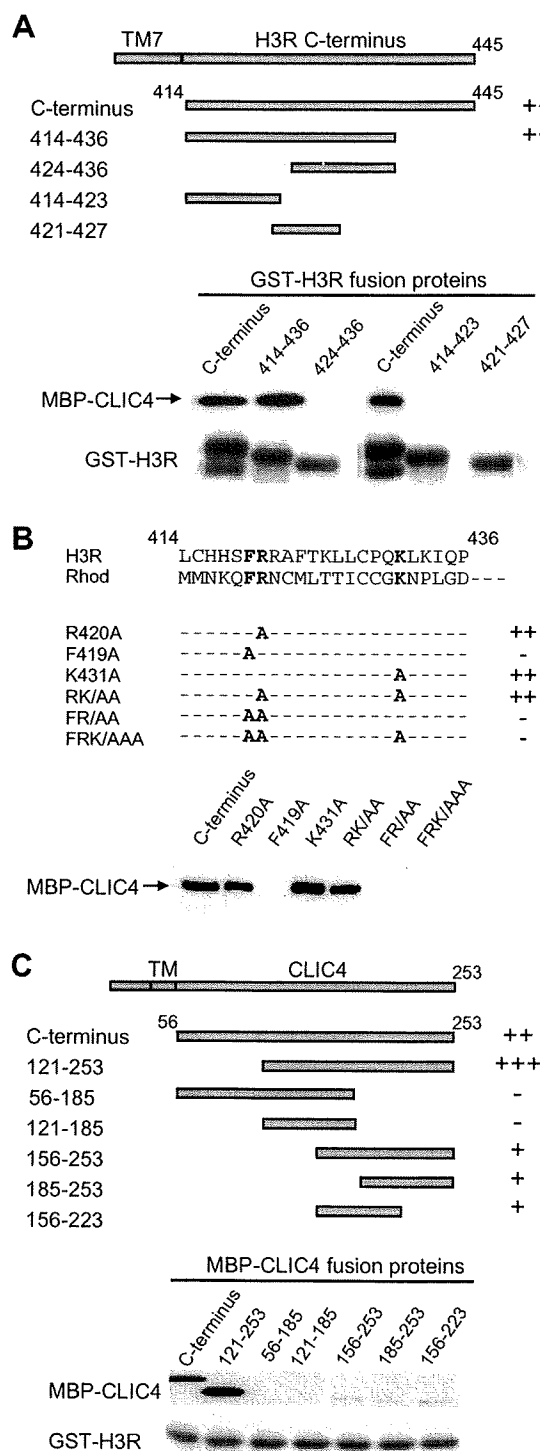


Fig. 1. Interaction of CLIC4 with H3R *in vitro*. Amino acid sequences responsible for the interaction between CLIC4 and H3R were determined. (A) Upper panel: Schematic diagram of full length C-terminal domain (414–445) and its distinct segments of H3R. Amino acid residue numbers, and binding activities with CLIC4 of each segment are indicated. Lower panel: Immunoblotting of MBP-CLIC4 coprecipitated with H3R and Coomassie blue staining of the samples. (B) Upper panel: Amino acid sequence alignment of H3R414–436 and C-terminus of rhodopsin (GenBank Accession Nos. NM_007232 and NM_000539). Boldface letters show amino acid residues replaced with alanines to generate mutant forms of H3R. Activities of each mutant to bind CLIC4 are indicated. Lower panel: Immunoblotting of MBP-CLIC4 coprecipitated with each mutant of GST-H3R. (C) Mapping of active subdomain of CLIC4 interacting with H3R. Upper panel: Schematic illustration of CLIC4(56–253) and its subsegments with their binding activities to H3R C-terminus. Lower panel: Immunoblotting detection of MBP-CLIC4 coprecipitated with H3R C-terminus, and Coomassie blue staining of the samples.

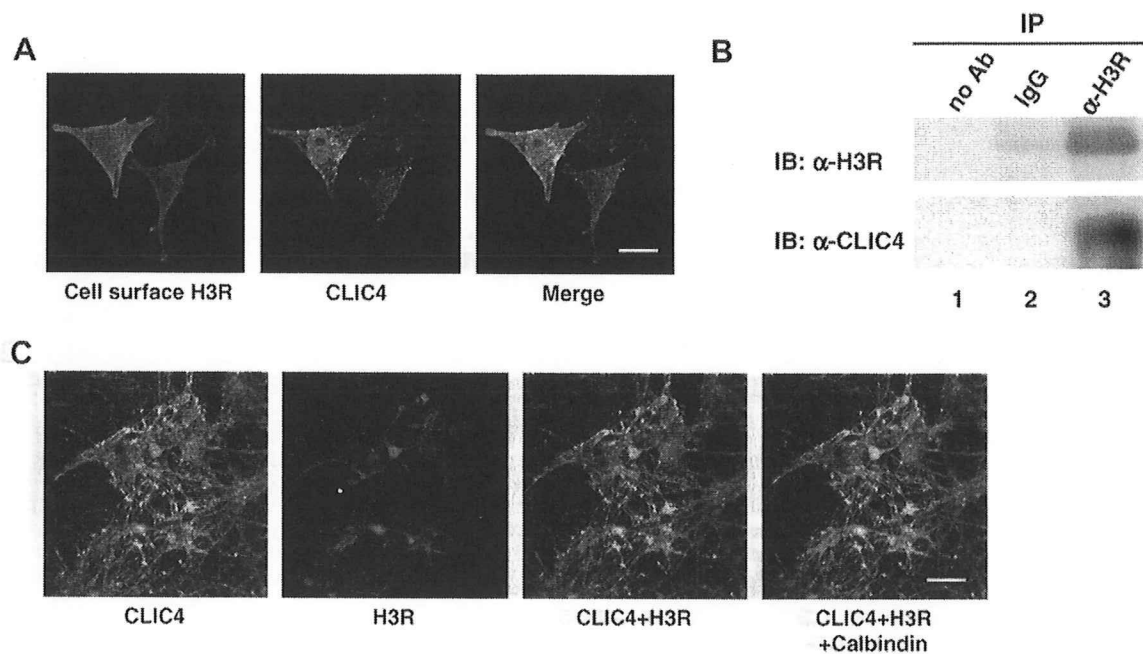


Fig. 2. *In vivo* association of CLIC4 with H3R. (A) Colocalization of CLIC4 and H3R at the plasma membrane of PC12 cells. Regions of colocalization of surface H3R and CLIC4 appear yellow in the merged image. Scale bar: 10 μ m. (B) Coimmunoprecipitation of endogenous CLIC4 with H3R. Solubilized proteins from rat brain P2 fraction were immunoprecipitated with no antibody (lane 1), irrelevant IgG (lane 2), or anti-H3R antibody (lane 3) and probed with anti-H3R or anti-CLIC4 antibodies. (C) Distribution of endogenous CLIC4 and H3R in rat cerebellar Purkinje cells. Cells were stained for H3R, CLIC4, and calbindin D-28K, a Purkinje cell-specific marker. Regions of colocalization of H3R and CLIC4 appear yellow and triple colocalization areas appear white in the merged image. Scale bar: 50 μ m.

(Fig. 2B). Furthermore, in immunofluorescence analysis of primary culture of rat cerebellar neurons, endogenous CLIC4 and H3R were colocalized in cell bodies and dendrites of Purkinje cells (Fig. 2C). These observations demonstrate that CLIC4 associates with H3R in native cells.

CLIC4 promotes cell surface expression of H3 receptor

To see whether CLIC4 alters the H3R trafficking in cells, cell surface H3R expression was examined by flow cytometry. PC12 cells were coinfecting with rAd-H3R and rAd-CLIC4, and cell surface H3R-derived fluorescence signals were measured. Fluorescence intensity was increased dose-dependently with simultaneous introduction of CLIC4 (Fig. 3A), indicating that increasing number of H3R was expressed on cell surface with the coexpression of CLIC4. Fluorescence signals measured in permeabilized cells indicated that the total amount of H3R in cells was not affected by CLIC4 (data not shown). We next investigated whether binding site of H3R specific ligand was altered by CLIC4. The [3 H]-RaMH specific binding showed progressive increase depending on the amount of rAd-CLIC4 used to infect the cells (Fig. 3B). We next performed saturation binding experiments with the radioligand. Scatchard plot analysis indicated that cells expressing H3R alone showed a single low-affinity binding site with a K_d value of 44.43 nM and a B_{max} value of 10.57 fmol/cell (Fig. 3C). On the other hand, cells expressing both H3R and CLIC4 displayed two distinct affinity sites

with K_d values of 0.99 nM and 94.55 nM, and B_{max} values of 2.71 fmol/cell and 17.24 fmol/cell for high- and low-affinity sites, respectively. Although the K_d value at the low-affinity sites has decreased more than 50% (from 44.43 nM to 94.55 nM), CLIC4 expression revealed new high-affinity sites on cells (K_d value of 0.99 nM) and increased nearly twice the total binding site density on cells (from 10.57 fmol/cell to 19.95 fmol/cell). We also investigated whether CLIC4 expression would influence cell surface expression of H3R in a different type of cells. Cell-based ELISA using CHO cells showed that cell surface expression of H3R was enhanced dose-dependently with simultaneous introduction of CLIC4 (Fig. 4A). It should be noted that the total amount of H3R detected in permeabilized cells was not influenced by CLIC4 (data not shown). This result indicates that the effect of CLIC4 is not restricted to a particular cell type but rather a more general attribute of CLIC4 to promote cell surface expression of H3R.

Surface expression of a mutant H3R is not enhanced by CLIC4

To confirm whether the specific interaction between H3R and CLIC4 is required for the increase in cell surface expression of the receptor, we investigated the effect of CLIC4 on the F419A mutant form of H3R that failed to interact with CLIC4. As demonstrated in Fig. 4B, the H3RF419A cell surface expression was

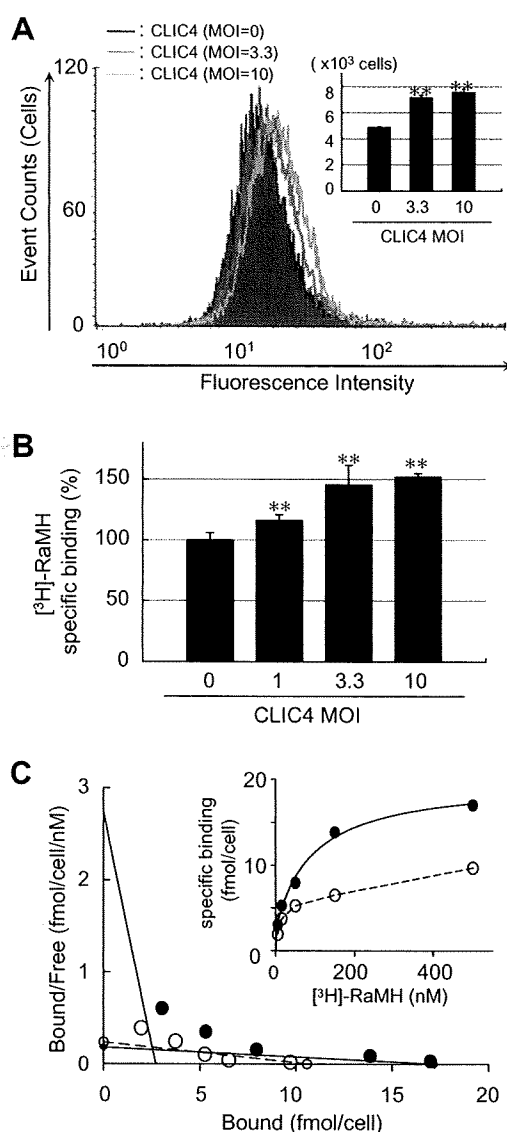


Fig. 3. Enhancement of H3R cell surface expression by CLIC4. (A) Effects of CLIC4 on H3R cell surface expression analyzed by flow cytometry. FACS analysis shows that fluorescence intensity derived from cell surface H3R was shifted to the right dose-dependently with simultaneous introduction of CLIC4. The inset shows a histogram of number of fluorescence-positive cells in each cell population. Data are shown in means \pm SE of three independent experiments. $**p < 0.01$ versus control. (B) Radioligand receptor assay. Specific binding of [³H]-RaMH was measured in PC12 cells coinfecting with rAd-H3R and rAd-CLIC4. Values were normalized to [³H]-RaMH binding to cells infected with only rAd-H3R. Each column represents the mean \pm S.E. of three independent experiments. $**p < 0.01$ versus control. (C) Scatchard plot of radioligand binding to H3R. Open circles indicate data from cells infected with only rAd-H3R. Closed circles denote cells coinfecting with rAd-H3R and rAd-CLIC4. The inset shows the saturation curve of [³H]-RaMH binding to the cells. Data are means of triplicate determinations.

not influenced by CLIC4. Basal level cell surface expression of the F419A mutant was comparable to that of the wild-type receptor (data not shown). This result strongly supports the idea that H3R cell surface expression enhanced by CLIC4 is caused by the specific interaction of H3R with CLIC4.

Discussion

Biosynthesis and fate of GPCRs are tightly coupled to the process of their trafficking within cells. After synthesized at ER, properly folded GPCRs are packaged into ER-derived vesicles and then conveyed to cell surface along the way through Golgi apparatus and trans-Golgi network (TGN). During the course of the transit to cell surface, GPCR molecules are post-translationally modified and assembled with effector signaling molecules including heterotrimeric G proteins. At the plasma membrane, GPCRs stimulated by their cognate ligands undergo internalization. Internalized receptors are carried through endosomes and then either degraded in lysosomes or recycled back to the plasma membrane. The number of GPCR molecules on the plasma membrane is defined by the balance of these processes of intracellular trafficking of the receptor. As H3R has been known to exhibit high constitutive activity [14], the receptor would be constitutively internalized even in steady state without ligand stimulation and recycled or degraded within cells. The ability of CLIC4 to enhance cell surface expression of H3R could, therefore, be explained by one or combinations of the following mechanisms: increase of forward trafficking of H3R from ER to cell surface, inhibition of constitutive receptor internalization, and increase of the receptor recycling back to the plasma membrane. CLIC4 is reported to interact with dynamin I [11], a protein essential in endocytosis. It is tempting, therefore, to speculate that CLIC4 expression would somehow influence activities of dynamin I, causing inhibition of the receptor internalization. As for the receptor recycling, endosome acidification is mandatory to maintain efficient vesicle recycling [15]. Proton transport required for the acidification of the endosomes should be balanced electrochemically with a concurrent chloride conductance of the vesicle membranes. Therefore, it would be conceivable that CLIC4 provides this conductance and enhances the recycling process of the constitutive active H3R. The third mechanism, increase of the forward trafficking of H3R, would also play a role in enhancing cell surface expression of the receptor.

Extensive studies on trafficking of GPCR have led to the identification of the structural determinants on the C-terminus of GPCR that dictate the efficiency of exit of the receptor from ER [16]. Among the several consensus motifs reported so far, F(X)₆LL (where X can be any residues and L is leucine or isoleucine) conforms to the CLIC4 binding site of H3R. The motif is reported to allow α_{2B} -adrenergic (α_{2B} -AR) and angiotensin II type 1 (AT1R) receptors to exit from ER [17]. The report also signifies the importance of the phenylalanine in this motif by showing that replacement of the residue with alanine causes both receptors to be unable to exit from ER. Because F419 of H3R is also critical for responding to CLIC4 enhancement of the receptor cell surface expression, it is intriguing to speculate that the protein responsible for binding this motif and assisting these receptors to exit from ER is CLIC4. However, a noticeable difference of H3R is that, unlike those mutants

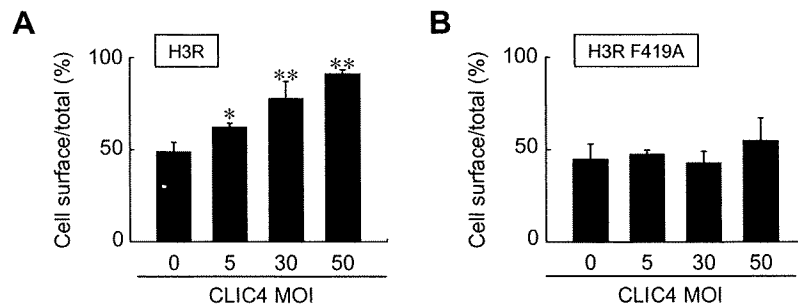


Fig. 4. Effects of CLIC4 on H3R cell surface expression in CHO cells. Cell surface H3R was measured by cell-based ELISA. (A) CHO cells were coinfecting with rAd-H3R and rAd-CLIC4, and cell surface and total cell H3R were determined. The percentage of cell surface H3R/total cell H3R are shown. * $p < 0.05$, ** $p < 0.01$ versus cells infected only with rAd-H3R. (B) CHO cells were infected with rAd-H3RF419A and rAd-CLIC4. Data are expressed as means \pm SE of three independent experiments.

of α_{2B} -AR and AT1R receptors with their phenylalanine residues replaced with alanines, the F419A mutant form of H3R is itself capable of exiting ER to be expressed on cell surface. This observation suggests that, for H3R to be trafficked to cell surface, some other protein is also operating during its transit from ER to cell surface that is insensitive to the F419 mutation.

Because the ligand binding affinity of GPCR would be defined generally by its three dimensional conformation and its state of association with heterotrimeric G proteins [5], CLIC4 might influence assembly of G protein signaling complex with H3R. Molecular mechanisms of G protein assembly with GPCR, and subcellular locations of the assembly sites along the trafficking route to the cell surface are poorly understood. Thus, it would be an interesting possibility that CLIC4 is a chaperon component of a GPCR trafficking machinery that operates at some location along the exocytic pathway where heterotrimeric G protein assembly takes place. It is also important to know if this unpredicted function of CLIC4 is shared among other members of CLIC protein family, and if any anion channel activity of the protein is essential to this function.

Acknowledgments

We thank Dr. C.H. Sung (Weill Medical College of Cornell University, New York) and Dr. T.W. Lovenberg (Johnson & Johnson Pharmaceutical Research and Development L.L.C., San Diego) for providing a human CLIC4 cDNA and a human histamine H3 receptor cDNA, respectively. We also thank Keiko Takahashi and Takako Maruyama for the exceptional technical assistance.

References

- [1] R. Leurs, R.A. Bakker, H. Timmerman, I.J. de Esch, The histamine H3 receptor: from gene cloning to H3 receptor drugs, *Nat. Rev. Drug Discov.* 4 (2005) 107–120.
- [2] S.J. Hill, C.R. Ganellin, H. Timmerman, J.C. Schwartz, N.P. Shankley, J.M. Young, W. Schunack, R. Levi, H.L. Haas, International Union of Pharmacology. XIII. Classification of histamine receptors, *Pharmacol. Rev.* 49 (1997) 253–278.
- [3] J. Bockaert, P. Marin, A. Dumuis, L. Fagni, The ‘magic tail’ of G protein-coupled receptors: an anchorage for functional protein networks, *FEBS Lett.* 546 (2003) 65–72.
- [4] M. Sugai, M. Saito, I. Sukegawa, Y. Katsushima, Y. Kinouchi, N. Nakahata, T. Shimosegawa, T. Yanagisawa, J. Sukegawa, PTH/PTH-related protein receptor interacts directly with Tctex-1 through its COOH terminus, *Biochem. Biophys. Res. Commun.* 311 (2003) 24–31.
- [5] D.J. Dupré, T.E. Hébert, Biosynthesis and trafficking of seven transmembrane receptor signalling complexes, *Cell. Signal.* 18 (2006) 1549–1559.
- [6] H. Singh, M.A. Cousin, R.H. Ashley, Functional reconstitution of mammalian ‘chloride intracellular channels’ CLIC1, CLIC4 and CLIC5 reveals differential regulation by cytoskeletal actin, *FEBS J.* 274 (2007) 6306–6316.
- [7] Y. Li, D. Li, Z. Zeng, D. Wang, Trimeric structure of the wild soluble chloride intracellular ion channel CLIC4 observed in crystals, *Biochem. Biophys. Res. Commun.* 343 (2006) 1272–1278.
- [8] R.H. Ashley, Challenging accepted ion channel biology: p64 and the CLIC family of putative intracellular anion channel proteins, *Mol. Membr. Biol.* 20 (2003) 1–11.
- [9] K.L. Berry, H.E. Bülow, D.H. Hall, O. Hobert, A *C. elegans* CLIC-like protein required for intracellular tube formation and maintenance, *Science* 302 (2003) 2134–2137.
- [10] S. Bohman, T. Matsumoto, K. Suh, A. Dimberg, L. Jakobsson, S. Yuspa, L. Claesson-Welsh, Proteomic analysis of vascular endothelial growth factor-induced endothelial cell differentiation reveals a role for chloride intracellular channel 4 (CLIC4) in tubular morphogenesis, *J. Biol. Chem.* 280 (2005) 42397–42404.
- [11] W. Suginta, N. Karoulias, A. Aitken, R.H. Ashley, Chloride intracellular channel protein CLIC4 (p64H1) binds directly to brain dynamin I in a complex containing actin, tubulin and 14-3-3 isoforms, *Biochem. J.* 359 (2001) 55–64.
- [12] J.Z. Chuang, T.A. Milner, M. Zhu, C.H. Sung, A 29 kDa intracellular chloride channel p64H1 is associated with large dense-core vesicles in rat hippocampal neurons, *J. Neurosci.* 19 (1999) 2919–2928.
- [13] N. Ilouz, L. Branski, J. Parnis, H. Parnas, M. Linial, Depolarization affects the binding properties of muscarinic acetylcholine receptors and their interaction with proteins of the exocytic apparatus, *J. Biol. Chem.* 274 (1999) 29519–29528.
- [14] J.M. Arrang, S. Morisset, F. Gbahou, Constitutive activity of the histamine H3 receptor, *Trends Pharmacol. Sci.* 28 (2007) 350–357.
- [15] K.M. Krueger, Y. Daaka, J.A. Pitcher, R.J. Lefkowitz, The role of sequestration in G protein-coupled receptor resensitization, *J. Biol. Chem.* 272 (1997) 5–8.
- [16] C. Dong, C.M. Filipeanu, M.T. Duverney, G. Wu, Regulation of G protein-coupled receptor export trafficking, *Biochim. Biophys. Acta* 1768 (2007) 853–870.
- [17] M.T. Duverney, F. Zhou, G. Wu, A conserved motif for the transport of G protein-coupled receptors from the endoplasmic reticulum to the cell surface, *J. Biol. Chem.* 279 (2004) 30741–30750.

Direct Injection of Kit Ligand-2 Lentivirus Improves Cardiac Repair and Rescues Mice Post-myocardial Infarction

Koji Higuchi¹, Bilal Ayach²⁻⁴, Takeya Sato⁵, Manyin Chen², Sean P Devine⁶, Vanessa I Rasaiah¹, Faye Dawood², Teruyuki Yanagisawa⁵, Chuwa Tei⁷, Toshihiro Takenaka⁸, Peter P Liu²⁻⁴ and Jeffrey A Medin^{1,2,4,6}

¹Division of Stem Cell and Developmental Biology, Ontario Cancer Institute, University Health Network, Toronto, Ontario, Canada; ²Toronto General Research Institute, University Health Network, Toronto, Ontario, Canada; ³The Heart and Stroke/Richard Lewar Centre of Excellence, University of Toronto, Toronto, Ontario, Canada; ⁴Institute of Medical Sciences, University of Toronto, Toronto, Ontario, Canada; ⁵Department of Molecular Pharmacology, Tohoku University Graduate School of Medicine, Sendai, Japan; ⁶Department of Medical Biophysics, University of Toronto, Toronto, Ontario, Canada; ⁷Department of Cardiovascular, Respiratory, and Metabolic Medicine, Graduate School of Medical and Dental Sciences, Kagoshima University, Kagoshima, Japan; ⁸Division of Cardiac Repair and Regeneration, Graduate School of Medical and Dental Sciences, Kagoshima University, Kagoshima, Japan

Myocardial infarction (MI) and subsequent adverse remodeling cause heart failure. Previously we demonstrated a role for Kit ligand (KL) in improving cardiac function post-MI. KL has two major isoforms; KL-1 is secreted whereas KL-2 is predominantly membrane bound. We demonstrate here first that KL-2-deficient mice have worse survival and an increased heart/bodyweight ratio post-MI compared to mice with reduced c-Kit receptor expression. Next we synthesized recombinant lentiviral vectors (LVs) that engineered functional expression of murine KL-1 and KL-2. For *in vivo* analyses, we directly injected these LVs into the left ventricle of membrane-bound KL-deficient *Sl/Sl^{fl}* or wild-type (WT) mice undergoing MI. Control LV/enGFP injection led to measurable reporter gene expression in hearts. Injection of LV/KL-2 attenuated adverse left ventricular remodeling and dramatically improved survival post-MI in both *Sl/Sl^{fl}* and WT mice (from 12 to 71% and 35 to 73%, respectively, versus controls). With regard toward beginning to understand the possible salutary mechanisms involved in this effect, differential staining patterns of Sca-1 and Ly49 on peripheral blood (PB) cells from therapeutically treated animals was found. Our data show that LV/KL-2 gene therapy is a promising treatment for MI.

Received 1 April 2008; accepted 10 June 2008; published online 11 November 2008. doi:10.1038/mt.2008.244

INTRODUCTION

Recent advances in understanding of the molecular mechanisms of cardiovascular disease, the role of stem cells in cardiac regeneration, and in gene delivery approaches allow thematic convergence for the development of novel treatments for heart disease. Although gene therapy has mainly been thought of as a treatment for cancer or inherited single-gene disorders, recent studies have

shown that this therapeutic approach has the capability to treat multifactorial diseases, including myocardial infarction (MI).^{1,2} Lentiviral vectors (LVs) are efficient gene delivery agents that have the capability to infect a variety of cell types including postmitotic cells. LVs have been approved for clinical utility and recent studies have demonstrated the use of these vectors in the treatment of cardiovascular disease.³

Adverse left ventricular remodeling post-MI triggers heart failure; it is important to prevent this outcome. Cytokine therapy post-MI is an attractive schema because such treatment might regenerate cardiac tissue and protect against adverse left ventricular remodeling.⁴⁻⁸ For example, Woldbaek *et al.* have shown that mRNA expression of Kit ligand (KL or SCF), the ligand for the steel receptor tyrosine kinase (c-Kit) receptor, is decreased in the heart post-MI.⁹ Furthermore, we have previously reported on detailed cardiac rescue and remodeling mechanisms post-MI involving the c-Kit receptor axis.¹⁰

KL has two isoforms, KL-1 and KL-2, which are formed by alternative splicing. KL-2 is missing a predominant extramembrane cleavage site¹¹ and is largely membrane bound. These two isoforms of KL have differential effects on the survival and proliferation of hematopoietic cells;^{12,13} observations which are reinforced by the altered phenotype of *Sl/Sl^{fl}* mice, which have only soluble KL. Importantly, membrane-associated KL has also demonstrated more potent and sustained signaling than its secreted counterpart.¹⁴

Recently, we reported α -galactosidase A correction in the hearts of animals in a Fabry disease model by direct intraventricular injection of a recombinant LV.¹⁵ That study on an inherited disorder provided a conceptual platform for the broadening of this therapeutic schema to impact acquired disorders as well. The aims of this present study were to develop novel recombinant LVs that engineer expression of KLs and to investigate the effects of direct left ventricular injection of vectors post-MI in mice. Effective vectors were generated and functional KL expression was documented *in vitro*. Direct injection of a LV that engineered

Correspondence: Jeffrey A. Medin, University Health Network, Room 406, 67 College Street, Toronto, Ontario, Canada. E-mail: jmedin@uhnres.utoronto.ca

expression of enGFP led to appreciable functional transductions of cardiac tissue. Next we observed that the overexpression of KL-2 by direct cardiac injection prevents adverse remodeling and dramatically improves survival post-MI both in KL-2-deficient mice and in wild-type (WT) animals. Increased survival was also correlated with differential expression of cell surface antigens Ly49 and Sca-1 on peripheral blood (PB) cells. These results open the door to the development of this therapeutic modality for the treatment of cardiovascular disease.

RESULTS

Decreased survival and worsened cardiac function in *Sl/Sl^d* mice post-MI compared with *W/W^v* mice

Our previous studies have shown that null *c-Kit* mutation *w/w^{viable}* (*W/W^v*) mice have diminished heart function and greater cardiac dilatation than WT mice 35 days after MI.¹⁰ We also demonstrated that these effects could be rescued by transplantation of WT bone marrow cells.¹⁰ To focus our present studies on dissecting the contributions of individual components of the KL/*c-Kit* receptor axis, we first performed MIs on *W/W^v* and *Sl/Sl^d* mice. *Sl/Sl^d* mice produce only soluble KL.¹¹ Figure 1 shows the results of preliminary studies providing survival percentages and heart/bodyweight ratio calculations measured at 5 weeks after MI. Clear differences were seen. *Sl/Sl^d* mice have markedly decreased survival percentages and an increased heart/bodyweight ratio in surviving animals at killing than *W/W^v* mice—indicating worsened outcomes post-MI.

KL overexpression in transduced *Sl/Sl^d* and TF-1 cells

Next, we developed novel LVs that engineer expression of KL-1 or KL-2 (LV/KL-1 and LV/KL-2, respectively). LV/KL-2 has an 84-bp deletion that removes the major proteolytic cleavage site; a minor cleavage site closer to the transmembrane domain is still maintained. LV/enGFP¹⁶ was used as a control *in vitro*. VSV-g-pseudotyped LVs were generated and titered as before.¹⁶ LVs were used to infect a KL-deficient murine stromal cell line, (*Sl/Sl^d* cells; ref. 17), at an MOI of 10. Nontransduced *Sl/Sl^d* cells were negative for KL expression while ~95% of infected cells expressed KL-1 and KL-2, respectively, as measured by flow cytometry analyses (Figure 2a). KL expression and protein relative molecular weights were confirmed by western blots performed on transduced *Sl/Sl^d* cell lysates (Figure 2b). Subsequently, the supernatant from pools of infected *Sl/Sl^d* cells was analyzed by ELISA to determine the concentration of cleaved KL (Figure 2c). As expected, more

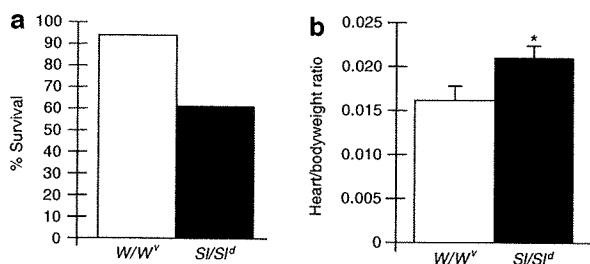


Figure 1 Comparison of functional outcomes in *W/W^v* mice ($n = 10$) and *Sl/Sl^d* mice ($n = 10$) that have undergone myocardial infarction (MI). (a) Percent survival measured at 5 weeks after MI. (b) Heart/bodyweight ratio of surviving animals measured at 5 weeks after MI. * $P < 0.05$.

secreted KL-1 was observed in similarly infected cells because of the inclusion of the major cleavage site. Finally, the bioactivity of KL generated by LV/KL-1 or LV/KL-2 infection was verified by its ability to support the growth of a KL-dependent cell line, TF-1 (ref. 18). Here transduced TF-1 cell pools were shown to proliferate faster than nontransduced cell pools, indicating production of functional KL (data not shown).

LV-mediated enGFP expression in infarcted hearts

To evaluate marking transgene expression mediated by a single LV administration in compromised recipients, WT mice received an MI-generating ligation and then phosphate buffered saline (PBS) or LV/enGFP were directly injected into their hearts in a minimal volume. Mice were killed 7 days after the MI. As expected, the enGFP signal was detected in the LV/enGFP-treated hearts and not in the PBS-treated hearts (Figure 3a,b). To avoid misleading outcomes due to possible autofluorescence, immunostaining was also performed for enGFP with a monoclonal antibody and then these signals merged with the enGFP fluorescence signals (Figure 3c–e). Relative fluorescence intensity was also calculated from a number of mounts of whole tissue samples derived from animals injected with serial dilutions of LV/enGFP. Figure 3f demonstrates, as could be predicted, that increased amounts of LV/enGFP injected leads to increased fluorescence intensity in cardiac samples. Finally, we also determined the relative cellular transduction rate from a number of fields for each mouse tissue mount (Figure 3g). These data indicate that ~5% of cells were functionally transduced by this direct LV injection method. Combined with our previous data,¹⁵ this indicates that this direct injection LV system is efficient for gene transfer into the heart.

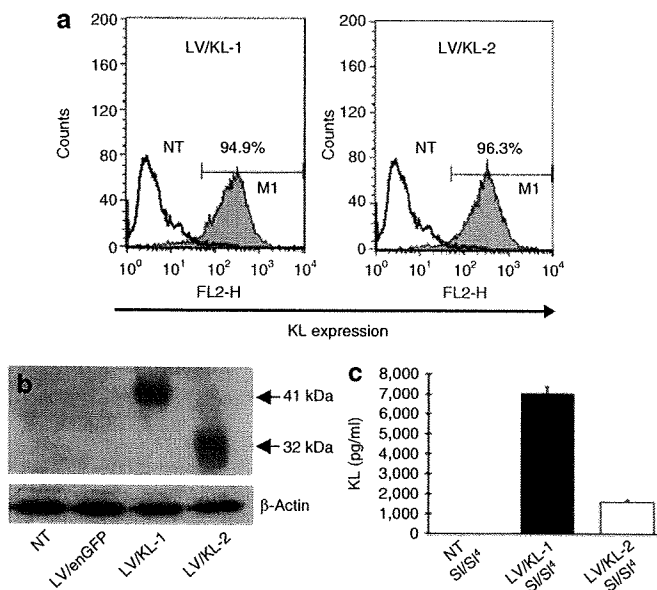


Figure 2 LV/KL-1 and LV/KL-2 efficiently infect *Sl/Sl^d* cells, a KL-deficient cell line. Transgene expression in infected cells was confirmed by (a) flow cytometry (KL expression in NT, LV/KL-1, and LV/KL-2 infected cells; 0.98%, 94.9%, and 96.3% respectively) and (b) western blot. For the western blot, LV/enGFP and nontransduced *Sl/Sl^d* cell extracts were used as controls. β -actin levels were evaluated as a protein loading control. (c) Cleaved KL in the supernatant of infected *Sl/Sl^d* cell pools was measured by ELISA. NT; nontransduced.

KL expression in the heart

To determine the effect of LV-mediated KL overexpression on recovery post-MI, our gene therapy strategy was tested in both *Sl/Sl^d* and in WT mice. These mice were randomized into six groups, receiving either MI or a sham operation. Within minutes after MI or sham operation, injection of the KL LVs was performed. Therapeutic transgene expression, mediated by direct vector injection, was then quantified. KL-2 expression was determined by ELISA from heart tissue of LV/KL-2-injected WT mice at 3 days after MI. KL-2 was observed to be overexpressed in the left ventricle of the LV/KL-2-injected hearts, including both the infarct and peri-infarct regions, compared to controls (Figure 4a). These results demonstrate that LV/KL-2 efficiently infects cardiac tissue from a single direct vector administration and generates KL-2 protein expression *in vivo*.

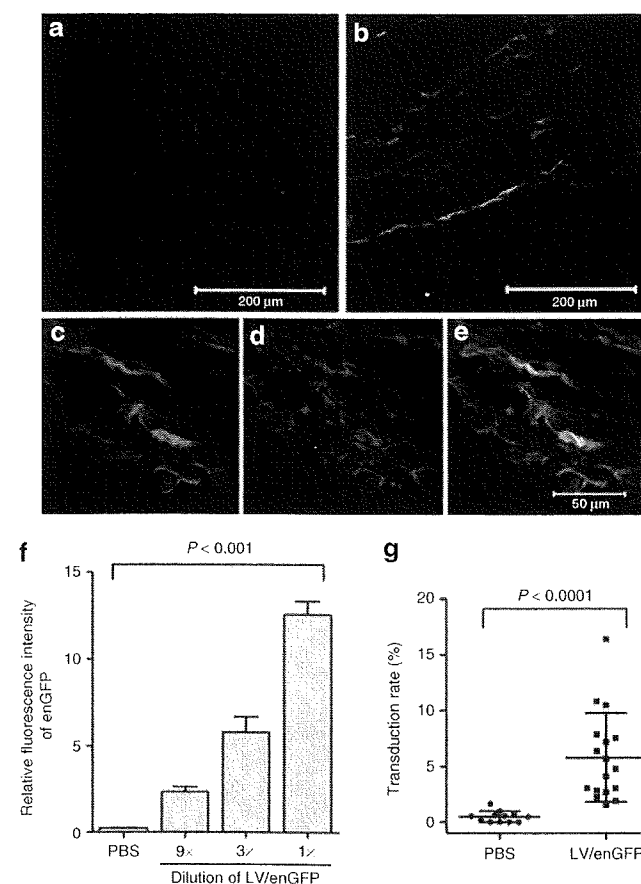


Figure 3 enGFP expression in the hearts of WT mice directly injected with LV/enGFP and receiving an MI. (a) PBS control-injected hearts and (b) LV/enGFP-injected hearts were examined for enGFP signal (green) and also stained with enGFP antibody (Alexa546, red). (c) enGFP signal at higher magnification. (d) Immunostaining for enGFP expression. (e) Overlay of c and d showing co-localization of the enGFP signal and enGFP staining. (f) Relative fluorescence intensity of the enGFP signal in hearts receiving direct injections of various doses of LV/enGFP. For each group 14 fields were analyzed per mouse injected ($n = 2$ or three animals per group). (g) Estimation of the transduction rate in cardiac tissue samples from LV/enGFP-injected mice. For the PBS-injected control group six fields were analyzed per mouse ($n = 2$ mice). For the LV-enGFP group 8 or 9 fields were analyzed per mouse ($n = 2$ mice).

LV/KL-2 administration substantially reduces infarct size and prevents adverse cardiac remodeling post-MI

Morphometric analysis was performed on injected WT mice at 7 and 35 days after MI. Representative results are shown in Figure 4b. In the LV/KL-2-treated group, left ventricular infarct sizes were significantly reduced ($37.2 \pm 2.5\%$ versus $59.3 \pm 3.0\%$, LV/KL-2 versus PBS respectively, $P < 0.001$) and left ventricular wall thickness was significantly improved at 35 days after MI (0.78 ± 0.24 mm versus 0.30 ± 0.03 mm, LV/KL-2 versus PBS respectively, $P < 0.05$) (Figure 4c,d).

Following cardiac remodeling post-MI, left ventricles are commonly dilated. In our study, we observed that the heart/bodyweight ratio in the LV/KL-2-treated group was significantly decreased compared with the PBS-treated group in WT mice ($0.0099 \pm 7.2 \times 10^{-4}$ versus $0.0123 \pm 6.8 \times 10^{-4}$, LV/KL-2 versus PBS respectively, $P < 0.05$) (Figure 5a). Furthermore, at 35 days after MI in WT mice, left ventricular end-diastolic volume and left ventricular end-systolic volume were reduced in LV/KL-1 and LV/KL-2-treated WT mice compared with PBS-treated WT mice (Figure 5b,c). These functional results show that LV/KL treatment prevented adverse cardiac remodeling in mice.

Direct LV/KL-2 injection markedly improves survival in *Sl/Sl^d* and WT mice post-MI

PBS-injected *Sl/Sl^d* mice demonstrated 12% survival at 35 days after MI (Figure 6a). In addition, animals receiving LV/KL-1 also had decreased survival frequencies (Figure 6a). In contrast,

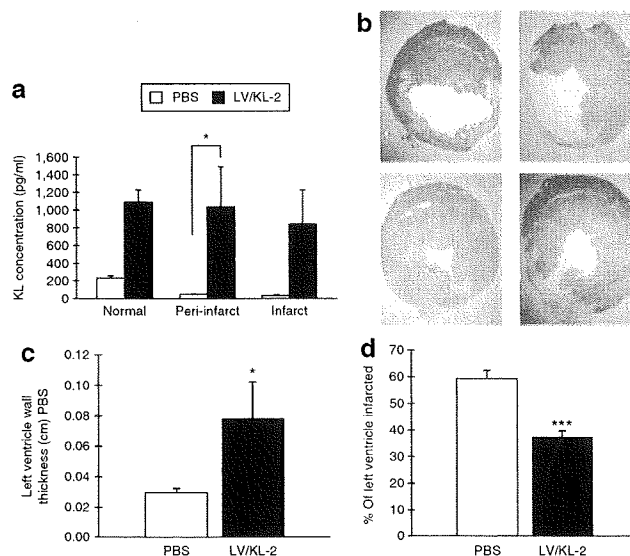


Figure 4 KL-2 expression in hearts and morphometric effects of LV/KL-2 gene therapy for MI. (a) Cardiac tissue KL expression as measured by ELISA at 3 days after MI in WT mice. Levels of KL are significantly greater in LV/KL-2-treated mice ($n = 3$) compared with PBS-treated mice ($n = 3$) in all areas of the heart. (b) Morphometrics (representative shown) demonstrate a smaller infarcted area in the left ventricle in LV/KL-2-treated WT mice compared with the PBS-treated group. (c) Left ventricular wall thickness and (d) the percent of left ventricle infarcted are significantly improved in LV/KL-2-treated WT mice ($n = 6$) at 35 days after MI compared with the PBS-treated group ($n = 6$). * $P < 0.05$, *** $P < 0.001$ compared with PBS-treated WT group.

survival was greatly improved in *Sl/Sl^d* mice treated with LV/KL-2, with 71% survival observed at 35 days ($P < 0.041$ versus PBS group) (Figure 6a). This result itself implicates the c-Kit receptor/KL axis as an important component of recovery post-MI and demonstrates that constructive manipulation of facets of that pathway can dramatically improve survival. Finally, we examined this therapeutic strategy in a more relevant model. We hypothesized that such robust repair mechanisms mediated by direct LV delivery of KL-2 could also work even in the context of existing normal recovery operations. Similar functional analyses were then performed in WT mice. Here we observed that survival of WT mice following MI was also significantly improved from 35 to 73.1% ($P < 0.05$) following LV/KL-2 treatment (Figure 6b).

Flow cytometric analyses of PB and immunohistochemistry from LV-injected and control mice post-MI

Toward gaining insights into mechanism, PB was obtained from surviving mice at days 0, 3, 7, 14, and 35 post-MI. MI is associated with a deleterious inflammatory response. Indeed, our previous results demonstrated that NK cells mediated cardiac survival and repair post-MI,¹⁰ therefore mononuclear cells were analyzed for expression of a directed series of cell surface markers including Ly49 (NK and NK-T cells), CD11c (NK, monocytes, macrophages, subsets of T and B cells), CD94 (NK, NK-T, activated CD8+ T cells), CD117 (c-Kit), CD34 (endothelial cells and short-term reconstituting HSCs), and Sca-1 (HSCs, activated lymphocytes).

Note that data from *Sl/Sl^d* mice receiving PBS post-MI could only be collected through 14 days because of high mortality. For some cell surface markers such as CD11c and CD34, values at day 35 were not different from starting values and were not dramatically impacted by the addition of LV/KL-2 (data not shown). This phenomenon also largely occurred with CD117 expression and CD94 expression (data not shown).

In contrast, for Ly49 expression starting values between the *Sl/Sl^d* and WT mice were quite similar (~5% of PB cells) as shown in Figure 7a. Yet at 14 days after MI these values started to diverge. Finally at 35 days both the *Sl/Sl^d* and WT mice receiving LV/KL-2 had significantly increased levels of Ly49⁺ cells in the PB ($8.1 \pm 2.4\%$ and $6.8 \pm 3.2\%$, respectively) in comparison with WT animals receiving PBS post-MI ($2.5 \pm 1.5\%$; $P < 0.006$) (Figure 7a).

Another class of responses were observed with the Sca-1 analyses. Concerning Sca-1, differences were seen in positive-staining percentages at baseline between WT and *Sl/Sl^d* animals at day 0 (~25% versus ~42%, respectively) (Figure 7b). These differences were largely maintained over the period of analysis. That is, except for those WT animals treated with the LV/KL-2. There at day 35, values for the WT animals treated with LV/KL-2 were dramatically different than those from animals treated with PBS only following MI ($39.2 \pm 13.5\%$ positive versus $20.2 \pm 11.0\%$ positive, respectively; $P < 0.034$). Further subset analysis of this group, *i.e.*, co-staining for Sca-1 and CD34 jointly, did not reveal differences in the numbers of cells dually positive for those markers, however (data not shown).

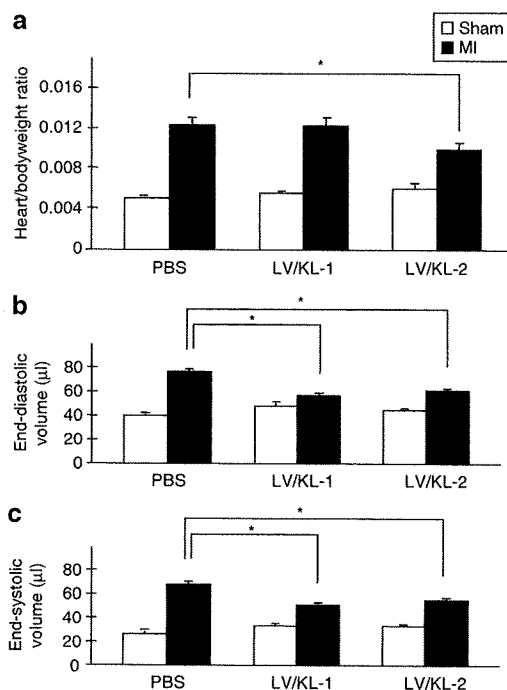


Figure 5 Physiological profiles following LV/KL-2 treatment for MI. LV/KL-2-treated WT mice ($n = 8$) demonstrate marked improvement in (a) Heart/bodyweight ratio, (b) left ventricular end-diastolic volume (LVEDP), and (c) left ventricular end-systolic volume (LVESV) compared with the PBS-treated group ($n = 3$). * $P < 0.05$, *** $P < 0.001$.

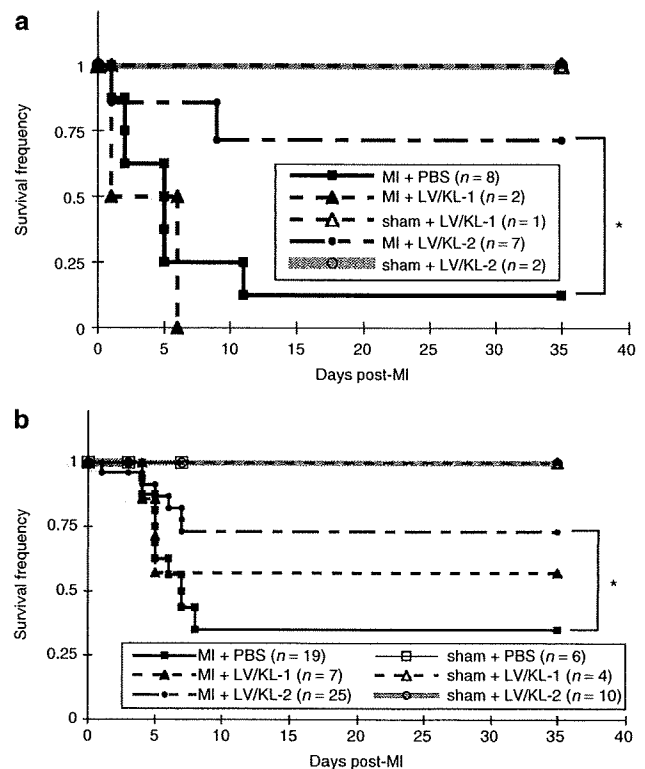


Figure 6 Direct LV/KL-2 injection enhances survival post-MI. LV/KL-2-treated (a) *Sl/Sl^d* and (b) WT mice demonstrate dramatically improved survival post-MI compared with PBS-treated mice. * $P < 0.05$, *** $P < 0.02$.

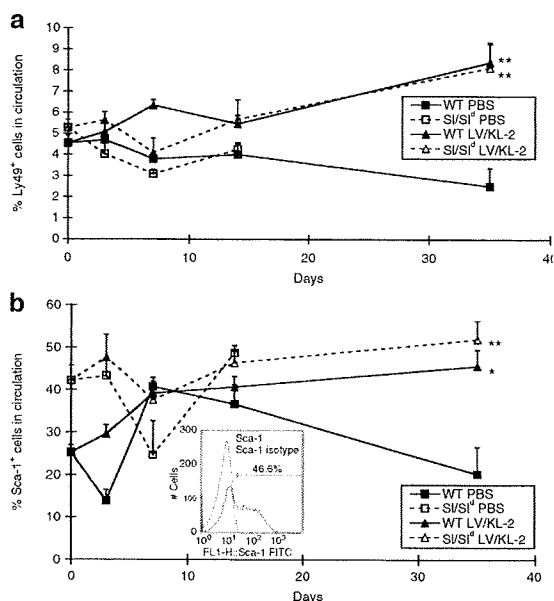


Figure 7 Results of flow cytometric analyses for Ly49 and Sca-1 staining of peripheral blood from WT and *Sl/Sf* mice treated with PBS or LV/KL-2 following MI. (a) Ly49⁺ cell mobilization over 35 days. (b) Sca-1⁺ cell mobilization over 35 days. Inset: Sample flow cytometry analysis for Sca-1 staining with isotype control. **P* < 0.05, ***P* < 0.01.

DISCUSSION

We have demonstrated that the LV gene delivery system is a promising approach for the treatment of MI; especially when the KL/c-Kit signaling axis (specifically KL-2) is accessed. LVs are able to transduce nondividing cells¹⁹ such as cardiomyocytes, integrate into the genome, and provide long-term transgene expression.²⁰ Indeed, Fleury *et al.* have shown efficient LV transduction and transgene expression *in vitro* in adult rat cardiomyocytes.²¹ Lower levels of sustained expression of KL-2 as generated by LV-mediated delivery may provide more benefit over time as repair is an ongoing process, compared to the higher bolus amounts of cytokines that would be produced using other transient delivery systems such as recombinant adenoviruses, for example. Outcomes from experiments designed to test this hypothesis would be interesting and provide further insights into mechanisms and timing of cardiac repair.

Our *in vitro* results demonstrate generation of effective recombinant LVs that drive expression of KLs. Our *in vivo* results demonstrate that LV-mediated KL-2 overexpression mediated by a single gene delivery event targeted directly into the murine myocardium dramatically improves hemodynamics and morphometrics (Figures 4 and 5, respectively) as well as survival of both KL-2-deficient and even WT mice post-MI (Figure 6). Indeed the robustness of this response is striking in the WT group given that normal signaling and repair pathways are still present in these animals. These results imply that membrane-bound KL is an important molecule in recovery and in prevention of adverse cardiac remodeling post-MI. These findings thus extend into the therapeutic realm results from our previous studies demonstrating the importance of systemic KL and c-Kit signaling in remodeling and rescue of the infarcted heart.¹⁰ Note that we have also performed studies with imatinib mesylate (Gleevec), which is a

pleiotropic agent that also blocks c-Kit function, and found a significant increase in animal mortality after MI over untreated animals (data not shown).

The mechanism whereby cytokine therapy prevents adverse cardiac remodeling has yet to be fully elucidated. It has been proposed that bone marrow cells are homing to the infarcted heart and transdifferentiate into cardiomyocytes post-MI.^{5,22,23} These cells may play an important role in cardiac remodeling post-MI. Recently, Dawn *et al.* have suggested that mobilization of cardiac stem cells themselves by cytokines could be an additional or alternative mechanism.^{8,24} Along these lines, it bears mentioning that we observed improved survival with LV/KL-2 compared to animals treated with LV/KL-1 (Figure 6a), although many fewer animals were tested in the second case. This may indicate a more pronounced requirement for the membrane-bound form of KL in cardiac rescue and remodeling post-MI, perhaps acting through an autocrine manner. These results may delineate a novel function for this isoform. On the other hand, we also show in Figure 2 that some detectable KL is secreted even from the form missing the major cleavage site. Thus perhaps both autocrine and paracrine mechanisms are at play here. In support of this hypothesis we see alterations in the nature of circulatory PB cells in treated animals (Figure 7). One difference between the two forms is in the duration and intensity of signaling, which is increased with KL-2 (ref. 14). KL-1 and KL-2 may also thus stimulate different homing or remodeling signals in this context.

For clinical application, further experiments need to be performed in order to address any pertinent safety concerns—such as any side effects with sustained overexpression of KL—and the optimal timing of vector administration following MI. Transcriptionally targeted vectors exploiting cardiac-specific promoters^{25,26} built into the next generation of recombinant LVs constructed for this purpose, for example, would decrease the likelihood of possible off-target expression effects. Likewise, the tropism of the vector may be made more restricted or the delivery system itself may be modified to further increase the potency of this approach. Concerning the timing of vector administration, these present proof-of-principle studies were undertaken wherein the MI and the vector delivery were performed immediately sequentially to address technical concerns and Animal Care Committee issues. Future studies, perhaps in rats (or other larger animal models) to relieve these concerns and optimize the timing of LV/KL-2 delivery to maximize beneficial outcomes following MI in the context of real world timing will be undertaken.

In summary, this is the first study to show improvement in survival using a novel direct LV gene therapy strategy and provides the platform for further development of this approach for potential treatment of MI.

MATERIALS AND METHODS

LVs. HIV-1 based recombinant LVs were constructed by replacing the enhanced GFP (enGFP) in pHR'-cPPT-EF-GW-SIN plasmid with the KL-1 or KL-2 cDNAs (LV/KL-1 or LV/KL-2). This construction method was previously described.¹⁶ The KL-1 cDNA was subcloned out from C57Bl/6 mice. Briefly, total RNA was isolated from stroma cells using the TRIzol reagent (Invitrogen, Carlsbad, CA). First strand cDNA was synthesized from 1 μ g total RNA using the SuperScript First Strand Synthesis System (Invitrogen). The specific KL-1 cDNA was amplified by PCR using primers

based on the published mouse KL-1 mRNA sequence (NM_013598). Forward primer: 5'-CGCTGCCTTTCCTTATGAAG-3' and Reverse primer: 5'-CGTCCACAATTACACCTCTTG-3'. KL-1 amplicons of ~850 bp were obtained after amplification for 35 cycles (denaturing at 94°C, 45 seconds; annealing at 57°C, 45 seconds; elongation at 72°C, 60 seconds) using Platinum Taq DNA polymerase High Fidelity reagents (Invitrogen). The mouse KL-1 cDNA product was subcloned using the PCR-Script Amp cloning Kit (Stratagene, La Jolla, CA).

KL-2 lacks the codon for exon 6 of the KL-1 sequence. To remove exon 6 from the KL-1 cDNA, inverse PCR was performed on the pPCR-Script/KL-1 plasmid template. The forward primer targeted the 3' end of exon 5 of the KL-1 cDNA and the reverse primer targeted the 5' end of exon 7 of KL-1 cDNA. Forward primer; 5'-CTTTCTCGGGACCTAATGTTG-3'; Reverse primer; 5'-GGAAAGCCGCAAAGGCC-3'. Inverse PCR was performed using Platinum Taq DNA polymerase High Fidelity reagents for 35 cycles. Each cycle consisted of the following steps: denaturation at 94°C, 30 seconds; annealing at 54°C, 5 minutes; extension at 68°C, 5 minutes each. The inverse PCR product was then self-ligated to make plasmid, which contains the KL-2 cDNA. This product (pPCR-Script/KL-2) was transformed into XL10-Gold Ultracompetent cells (Stratagene) and verified by DNA sequencing.

Vesicular stomatitis virus glycoprotein-pseudotyped (VSV-g) LVs, including an enGFP control vector (LV/enGFP) used *in vitro*, were generated by transient transfection of 293T cells (obtained from Michele Calos, Stanford University) using the three-plasmid system (LV plasmid construct, packaging plasmid pCMV Δ R8.91, and the VSV-g envelope-coding plasmid pMD.G) with FuGENE6 (Roche, Indianapolis, IN). Virus supernatant were harvested at 48 hours and concentrated at 50,000g for 2 hours. The concentrated viral supernatants were serially diluted and titered on 293T cells. p24 antigen levels also were determined by an HIV-1 p24 ELISA (PerkinElmer, Waltham, MA).

Functional expression of KL transgenes in the Sl/Sl⁴ and TF-1 cell lines. The Sl/Sl⁴ cell line was purchased from ATCC (Manassas, VA). Sl/Sl⁴ cells were cultured in Dulbecco's Modified Eagle Medium with 10% fetal bovine serum, 100 IU of penicillin/ml and 100 μ g of streptomycin/ml. A half million Sl/Sl⁴ cells were infected a single time with LV/KL-1, LV/KL-2, or LV/enGFP at an MOI of 10 in the presence of 8 μ g/ml protamine sulfate. Flow cytometric analyses were performed 2 days later. Transduced Sl/Sl⁴ cells were also lysed in sample buffer and cell lysates were resolved by SDS-PAGE and transferred onto polyvinylidene difluoride filters (Millipore, Billerica, MA). Filters were blocked with 10% skim milk in PBS with 0.1% Tween20 for 1 hour at RT. KL was detected with biotinylated anti-mouse KL antibody (BAF455; R&D Systems, Minneapolis, MN), used at 0.2 μ g/ml. Equal protein loading was confirmed with an anti- β -actin antibody (A5441; Sigma Aldrich, St Louis, MO) diluted 1:10,000. Blots were probed with secondary anti-goat (diluted 1:5,000, sc-2020; Santa Cruz Biotechnology, Santa Cruz, CA) or anti-mouse (diluted 1:1,000, NA931; GE Healthcare, Piscataway, NJ) horseradish peroxidase-conjugated antibodies. Protein bands were detected using an enhanced Chemiluminescence kit (Perkin Elmer, Waltham, MA).

Transduced or nontransduced Sl/Sl⁴ cells were seeded in a 10-cm dish in 10 ml of DMEM with 10% fetal bovine serum. Supernatant was harvested 2 days later and KL concentration was measured using the SCF ELISA kit (R&D Systems).

TF-1 cells, which are a human erythroblast cell line, were obtained from ATCC. TF-1 cells were infected with LV/KL-1 and LV/KL-2 at an MOI of 5. Three days after transduction, infected TF-1 cells were harvested and the cells were washed with PBS twice. TF-1 cells were incubated with biotinylated anti-mouse SCF antibody (R&D Systems) at 4°C for 20 minutes and washed twice with PBS. These cells were incubated with streptavidin-phycoerythrin (BD Biosciences, San Jose, CA) at 4°C for 20 minutes and washed with PBS twice. Expression of KL-1 and KL-2 on infected TF-1 cells was determined by flow cytometry and found to be 68.9 and 49.2%, respectively (data not shown).

Experimental animals. WBB6F1/J-Kit^W/Kit^{W-v} (W/W^v) mice, WCB6F1/J Kit^{Sl} kit^{Sl-d} (Sl/Sl^d) mice, and their littermates (WT) were purchased from the Jackson Laboratory (Bar Harbor, ME). Animal experiments were performed under protocols approved by the University Health Network Animal Care Committee.

Induction of MI and cardiac injection of LVs. MI was induced by permanent ligation of the left anterior descending coronary artery as described previously.²⁷ Forty microliters of LVs (corresponding to 2.8 μ g/ml p24 antigen) or PBS were injected into the left ventricle as before.¹⁵

In vivo study plan. In experiment 1, Sl/Sl^d ($n = 20$) and WT ($n = 37$) mice were randomized into six groups. Mice received either an MI or sham operation and then PBS or LVs encoding KL-1 or KL-2 were injected directly into the left ventricle. Mice were monitored for morbidity and mortality. The percentages of death from the MI/injection procedure itself and controls, in Sl/Sl^d+MI, Sl/Sl^d+sham, WT+MI, and WT+sham groups, were 52.9, 50, 10.5, and 4.8%, respectively. At 35 days after MI, mice were killed after the evaluation of cardiac function. In experiment 2, WT mice ($n = 34$) were subjected to MI or sham operation and PBS or LV/KL-2 were injected. Some mice were randomly killed for analyses on 3, 7, and 35 days after MI.

In experiment 3, to check the efficiency of LV-mediated gene transfer into the heart, WT mice received an MI operation and were injected with PBS or LV/enGFP ($n = 3$ for each group) and were killed for immunohistochemistry 7 days after MI.

Flow cytometric analyses and antigen retrieval staining. PB was collected at 0, 3, 7, 14, and 35 days after MI. Cell surface expression of marker proteins on PB cells were analyzed by flow cytometry. Twenty microliters of PB cells were lysed with Red Blood Cell Lysing Buffer (Sigma) and incubated with antibody against Ly49, CD11c, CD94, CD117, Sca-1, and CD34 (all antibodies were purchased from BD Biosciences). PB cells were analyzed on a FACSCalibur flow cytometer (BD, Franklin Lakes, NJ).

To perform antigen retrieval staining for enGFP, heart sections were incubated in HistoVT One (Nacalai Tesque, Kyoto, Japan) for 20 minutes at 70°C. The tissues were permeabilized with PBS-T (0.1% Triton X-100 in PBS). The sections were incubated with anti-GFP monoclonal antibody (Nacalai Tesque, clone GF090R), and subsequently incubated with Alexa546-labeled goat anti-rat IgG antibody (Molecular Probes, Eugene, OR).

Cardiac function and morphometric evaluation. Cardiac function was analyzed using a Millar pressure volume conductance catheter. Morphometrics were analyzed as described before.²⁷ Briefly, hearts were harvested, rinsed with PBS, and embedded in OCT. Tissue was sectioned at 5 μ m and stored at -80°C until analysis. Digitally captured pathological images were used to evaluate the left ventricular area, wall thickness, and percent-infarcted area.

Statistical analyses. All statistical analyses were performed using a two-sample Student's *t*-test assuming unequal variance. For Kaplan-Meier curves, a logrank test was used to evaluate significance.

ACKNOWLEDGMENTS

This work was supported, in part, by the Heart and Stroke Foundation of Ontario and the Canadian Institutes of Health Research. We thank Makoto Yoshimitsu (Kagoshima University) for invaluable assistance.

REFERENCES

1. Sasano, T, McDonald, AD, Kikuchi, K and Donahue, JK (2006). Molecular ablation of ventricular tachycardia after myocardial infarction. *Nat Med* **12**: 1256-1258.
2. Kusano, KF, Pola, R, Murayama, T, Curry, C, Kawamoto, A, Iwakura, A *et al.* (2005). Sonic hedgehog myocardial gene therapy: tissue repair through transient reconstitution of embryonic signaling. *Nat Med* **11**: 1197-1204.